OPTIMIZATION OF INTENSITIES AND LOCATIONS OF DIFFUSE SPOTS IN INDOOR VISIBLE LIGHT OPTICAL WIRELESS COMMUNICATION SYSTEM

BY

ABDULLAHI, Babadoko Baba

MENG/SEET/2018/8109

DEPARTMENT OF TELECOMMUNICATION ENGINEERING

FEDERAL UNIVERSITY OF TECHNOLOGY MINNA

APRIL, 2023

OPTIMIZATION OF INTENSITIES AND LOCATIONS OF DIFFUSE SPOTS IN INDOOR VISIBLE LIGHT OPTICAL WIRELESS COMMUNICATION SYSTEM

BY

ABDULLAHI, Babadoko Baba

MENG/SEET/2018/8109

A THESIS SUBMITTED TO THE POST GRADUATE SCHOOL, FEDERAL UNIVERSITY OF TECHNOLOGY, MINNA IN PARTIAL FULFILLMENT FOR THE AWARD OF THE DEGREE OF MASTER OF ENGINEERING IN COMMUNICATION ENGINEERING

APRIL, 2023

DECLARATION

I hereby declare that this thesis titled **"Optimization of Intensities And Locations of Diffuse Spots in Indoor Visible Light Optical Wireless Communication System**" is a collection of my original research work and it has not been presented for any other qualification anywhere. Information from other sources (published or unpublished) and their contributions has been duly acknowledged**.**

ABDULLAHI, Babadoko Baba
MENG/SEET/2018/8109
FEDERAL UNIVERSITY OF TECHNOLOGY
MINNA, NIGERIA

SIGNATURE/DATE

CERTIFICATION

The thesis titled "OPTIMIZATION OF INTENSITIES AND LOCATIONS OF DIFFUSE SPOTS IN INDOOR VISIBLE LIGHT OPTICAL WIRELESS COMMUNICATION SYSTEM " by ABDULLAHI, Babadoko Baba MENG/SEET/2018/8109 meets the regulations governing the award of the degree of MTech of the Federal University of Technology, Minna and it is approved for its contribution to scientific knowledge and literary presentation.

Engr. Dr. David Michael **Signature& Date**
MAJOR SUPERVISOR

Engr. Dr. Suleiman Zubair **Signature & Date**
CO - SUPERVISOR

Engr.Dr. A. U. Usman **Signature & Date**
HEAD OF DEPARTMENT

Engr. Prof. E. N. Onwuka **Signature & Date**
DEAN SCHOOL OF ELECTRICAL
ENGINEERING AND TECHNOLOGY

Engr. Prof. O. K. Abubakre **Signature & Date**
DEAN OF POSTGRADUATE
SCHOOL

DEDICATION

This work is dedicated to THE ALMIGHTY ALLAH, who knows everything and do everything.

ACKNOWLEDGEMENTS

Allah is the Greatest, To Allah we shall return all the Glories. I sincerely thanked God Almighty for the opportunity to undergo this program “Masters of Engineering in Communication Engineering Technology” I must also thank those God used for the actualization of the aforementioned goal as follows:

My main supervisor in person of Engr. Dr. Michael David, Co- Supervisor Engr. Dr. Suleiman Zubair and all lecturers of Telecommunication Department, School of Electrical Engineering Technology, Federal University of Technology Minna, thank you all for the guidance and other support services.

My family members, especially my lovely spouse Mrs. Rashidat Abdullahi Babadoko for her patience and encouragement, Sister Taiwo A Maidalailu for her support in cash and kindness, my father Mohammed Abdullahi Baba, Ahmed Gimba (Alhaji) and all other family members for their prayers. Computer operators and engineers both at Federal University of Technology Minna, College of Education Minna and Obasanjo complex Minna for helping me in the following areas; Soft wares installation, repairs and maintenance of my computer system and for guiding me in the operation of the system in general.

ALHAMDULILAH! ALHAMDULILAH!! ALHAMDULILAH!! After every difficulty is relieved

TABLE OF CONTENT

LIST OF TABLE

LIST OF FIGURE

LIST OF ABREVIATIONS

CDMA– Code division multiple access

DS - Delay spread

DiSs - Display or Diffuse spot

FoV - Field of view

IM/DD – Intensity modulation and direct detection

IoT- Internet of things

IRC - Infrared light communication

ISI – Inter Symbol interference

LAN – Local area network

LED – Light emitting diode

MIMO – Multiple Input /Multiple Out put

OF – Optical frequency

OFDM – Orthogonal frequency division multiplexing

OI – Operational intelligence

OWC – Optical wireless communication

PAPR – Peak to average power ratio

PSO – Particles swarm optimization

RC – Repetition coding

RF – Radio frequency

RMS – Root mean square

RSS – Received signal strength

RX – Receiver

SDN – Software defined network

SNR – Signal to noise ratio

Tx – Transmitter

ULC – Ultraviolet light communication

VLC – Visible light communication

3D – Three dimension

5G – Fifth generation network

5GB - Fifth generation network and beyond

6G – Sixth generation network

Lifi – Light Fidelity

Wifi – Wireless Fidelity

ABSTRACT

This research focused on the optimization of spread photo-signals parameters (diffuse spots' parameters) in indoor Optical Wireless Communications (OWC) system. Since line of sight nature of optical signals makes it difficult to be utilized effectively, while future wireless communication is expected use to both Radio Frequency (RF) and Optical Frequency (OF) simultaneously to complement each other's drawbacks. Hence, this research is to solve the problem of blockage of light signals, it was carried out by employing both JAYA optimization algorithm and Particle Swarm Optimization (PSO) algorithm, comparison was made with the other work which uses only PSO Optimization algorithm the outcome gave birth to different optimization scenarios and a model of optimized intensities and locations of light signals. This research work on maximizations/minimization simultaneously optimized the scattered photo-signals (diffusion spots') locations and intensities, an improvement in the Signal-to-Noise-Ratio (SNR) and the delay spread at the receivers were shown, also considering both the background noise and the multipath dispersion. This research illustrates the effect of varying the parameters that are being optimized. The results show that the optimization of both intensities and locations of scattered photo-signals (diffuse spots) resulted into an improvement of up to 29% and 23.3% in the Average Signal-Noise-Ratio (SNR) and Average Delay Spread, respectively, when compared to the centrally located position of diffuse spots' (circular photo-signals) distribution, with respect to the receiver's locations, which has a uniform distribution of power. The outcome of the optimized model can be used in indoor high speed connectivity for efficient data transfer.

CHAPTER ONE

1.0 INTRODUCTION

1.1 Background to the Study

In the past few years, the demand for high data rate services has increased tremendously. The congestion in the radio frequency (RF) spectrum (3 kHz ~ 300 GHz) is expected to limit the growth of future wireless systems unless new parts of the spectrum are opened. Even with the use of advanced engineering, such as signal processing and advanced modulation schemes, it will be very challenging to meet the demands of the users in the next decades using the existing higher sine waves frequencies(Alsulami *et al,* 2018). On the other hand, there is a potential band of the spectrum available that can provide tens of Giga bit per second to Terra bit per second (Gbps to Tbps) for users in the near future for the proposed 5G & 6G wireless communication networks. Optical wireless communication (OWC) systems are among the promising solutions to the bandwidth limitation problem faced by radio systems(Agiwal *et al* 2016). OWC systems that operate at short ranges such as indoor systems are prone to some challenges such as (a) skin and eye safety regulations (b) Inter Symbol Interference and (c) signal corruption due to intense ambient light or/and sunlight (i.e background noise). OWC systems is an unregulated spectrum communication channel as such it is unlicensed, DC bias elimination, PAPR penalty especially using IM/DD technique and the cost can be reduced compared to licensed RF systems, all these make OWC attractive.

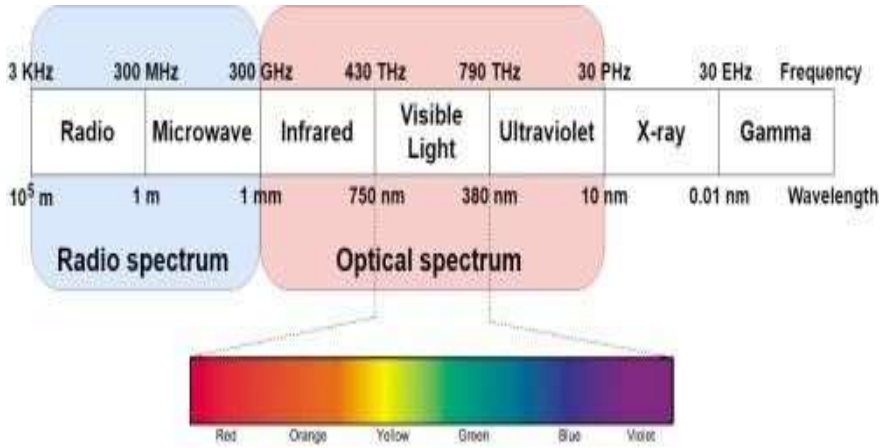

Figure 1.1: The Electromagnetic Spectrum.

1.2 Motivation

The nature of light gives OWC systems immunity against interference caused by adjacent channels in neighboring rooms, with the possibility of frequency reuse in different parts of the same building, which means increased capacity, low cost and increased bandwidth among other benefits.

OWC systems also offer better security at the physical layer. This is due to the fact that light does not penetrate opaque barriers, which means the potential for eavesdropping is reduced unlike in radio systems, and this reduces the need for data encryption (Kirrbach *et al.* 2019).

In addition, the detector (photodiode) has a very large area, typically tens of thousands of wavelengths, and this leads to efficient spatial diversity at the receiver (Akpakwu *et al.* 2017). These combined favorable features make OWC systems suitable replacements for conventional radio systems (Alsulami *et al*. 2018).

1.3 Statement of Research Problem

The area of wireless communications is facing major transformations as the mobile communication is transitioning to the fifth-generation technology while local area networks to the sixth-generation of Wi-Fi. RF is becoming saturated (Zadobrischi *et al.* 2019) in which cooperation between various technologies in a hybrid platform is foreseen as solutions to the increasing demands and requirements from human users and internet of thing (Javaid *et al.* 2021). Optical Wireless Communication (OWC) systems have potential to provide high data rates and support multiple users simultaneously by integrating RF with visible light communication(VLC) in indoor scenario in order to boost speed and suppress latency(Chowdhury and Hasan 2019). Since increased in capacity accompanied by saturated RF slower data transfer rate (Zadobrischi *et al.* 2019). According to (Eltokhey *et al.* 2019) higher data rates can be investigated by Optimizing the intensities and locations of different components/ parameters to achieve higher data rate through improved Signal to Noise Ratio (SNR) and compressed Delay Spread this formed the basis of motivation of this research work.

1.4 Aim and Objective

To Optimize the intensities and locations of diffused spots while varying indoor OWC parameters to have an improvement in data rate achieved in the existing systems by maximizing and minimizing signal-to noise-ratio (SNR) and the delay spread respectively at the receivers.

The aim of this research work is achieved through the following objectives:

i. To design an indoor optical wireless communication system of a transmitter, receiver, noise sources, and a feedback channel.

ii. To Optimize the diffusion spots' locations and intensities, using both JAYA and Particle Swarm Optimization(PSO)

iii. To evaluate the performance of the developed model in ii above and establish improvement in bit rate rate already achieved in (Eltokhey 2019) through simulation with the aid of matlab

1.5 Justification of the Study

Several authors that proposed the use of Non Line of Sight/ Diffuse spot channel in indoor optical wireless communication systems had results of Bit rate less than or equal to 50MB/s (Stassen and Colak 2020)

While Other authors use LOS to achieved more Bit rates but with more complexity in the systems, non-mobility and at higher cost (Chun *et al.* 2019). Visible Light Communication(VLC) is used for both lightening and communication was justified by Arfaoui *et al.* (2020).

It was also proved by Manousiadis *et al.* (2020) that "Organic semiconductors have considerable potential as color converters in lighting, not only because they can implement more efficient white-light VLC links, but also because they can provide high-quality light cheaply, and without dependence on the rare-earth elements in inorganic phosphors". Most of the reported high speed visible-light systems though have shown fixed point-to-point links with limited coverage. They used a simple direct modulation and detection and relatively cheap silicon receiver to achieve the maximum reported data-rate of ~10 Gb/s. The biologically friendly visible wavelength systems can provide lighting function for diffuse spot configuration link in indoor systems for better performance and cost effective through optimization.

1.6 Significance of the Research

According to (Khalighi *and* Ghassemlooy. 2021), future wireless network requirements are most likely to be satisfied with the help of hybrid communication technologies rather than by unique solutions, hence some merits of OWC systems are unlicensed spectrum, high transmission bandwidth, inherent security, absent of interference based on radio frequency, and the ability to use the same wavelength (frequency reuse) within a room or an entire building make OWC an attractive and complementary candidate to the radio frequency based wireless technologies in a number of applications such as intra-vehicular communications, wireless sensor networks, healthcare monitoring, and others *(Eltokhey et al. 2019)* and the provision of an uplink connection for VLC systems. In another development the total data traffic is expected to surpass about 49 exabytes per month by 2021, while in 2016, it was approximately 7.24 exabytes per month. With this drastic increase, the fifth generation (5G) networks and beyond must urgently provide high data rates, seamless connectivity, robust security and ultra-low latency communications (Arfaoui *et al.* 2020). However, traditional radio-frequency (RF) networks, which are already congested, are unable to satisfy these high demands. Network densification has been proposed as a solution to increase the capacity and coverage in 5G networks (Abhishek *et al*. 2020) The vision for the fourth-generation (4G) and fifth-generation (4G) wireless communication systems sets the peak download speed at 100 Mb/s for high-mobility communication and 1 Gb/s for low-mobility communication (Elgala *et al*, 2011). In this thesis, OWC system (VLC Diffuse Spot Link) design modification will be carried out, simulated and optimized intensities to increase SNR to have an improved data transfer rate that suit present demands (Wu *et al.* 2012).

CHAPTER TWO

2.0 LITERATURE REVIEW

In this section, we look at various literatures that worked on optical wireless communications, how to improve data transfer rate using optical wireless communication systems, safety of data and emerging hybrid technologies in both RF wireless systems and optical wireless systems This section will be sub-divided into segments namely; (i) General Review and (ii) Optical Review.

Optical wireless communication systems also have some draw backs such namely;

(a) Infrared light communication (IRC) most of the Infrared beam-steering systems reported higher data-rate using relatively complex methods such as high bandwidth external modulation, polarization control and high sensitivity InGaAs receivers often with optical amplifiers (Chun *et al.* 2019).

(b) Light Fidelity Optical Communication System this system covers a relatively short range, usually a few meters with a single access point and is susceptive to connectivity loss due to obstructions (Jatau *et al,* 2020). Hence, as a complementary approach to wireless network technology (WiFi), LiFi is a promising technology to fulfill the future demand for data rates but also with some challenges (i.e Integration of Radio Frequency and Optical Frequency) (Xiping *et al.* 2020; Jatau *et al* 2020).

Hence, Infrared light communication and Visible light communication LEDs are used to optimize the diffusion spots' locations and intensities, we shall show an improvement in the signal-to noise-ratio (SNR) and the delay spread at the receivers, while considering both the background noise and the multipath dispersion. A comparison is proposed between

different optimization scenarios. Recently, infrared and visible light have gained ground with operators seeking to cover area that require high bit rate services such as the office areas. Serious work on indoor optical wireless systems started during early 90s for IRC and for VLC it was mid 2000's (Lebaka 2006).

At present it is a very rapidly developing research area and there is huge interest and commitment in this area by major communication industries due to its enormous commercial applications(Vincent *et al*. 2017) In conventional Visible Light Positioning, light intensity is generally captured by either a photodiode (PD) or a camera.

When using a PD, one can use the photocurrent to determine the distance to the transmitters via a signal strength model (Cosovanu and Done 2020). This method is relatively straightforward, yet sensitive to fluctuations in light intensity, which can occur for example with dimming and alternatively, one can also use time of flight or round trip time to obtain the transmitter–receiver distance(Amsters *et al* 2019). It was shown in (Zou *et al* 2016) that it is possible to generate secret bits at a sufficiently high rate based on the wireless channel variations in highly dynamic mobile scenarios.

However, one of the major limitations of optical wireless networking technologies is the inherent line of sight (LOS) nature of optical carriers. To overcome this obstacle a number of solutions have been proposed, which can be distinguished into diffuse and spot diffusing techniques *(Xiping et al. 2020).*

In the propagation of the diffused spot link, after some reflections the irradiance is almost uniform, so that detector need not be oriented towards the transmitter. Full mobility within the room is allowed and there are no shadowing effects caused by moving persons or machines

(Lebaka, 2006).

Hence, the optical power has to be high to cover the entire room, and multipath dispersion limits the data rate. Multipath propagation causes a spread of transmitted pulse, which

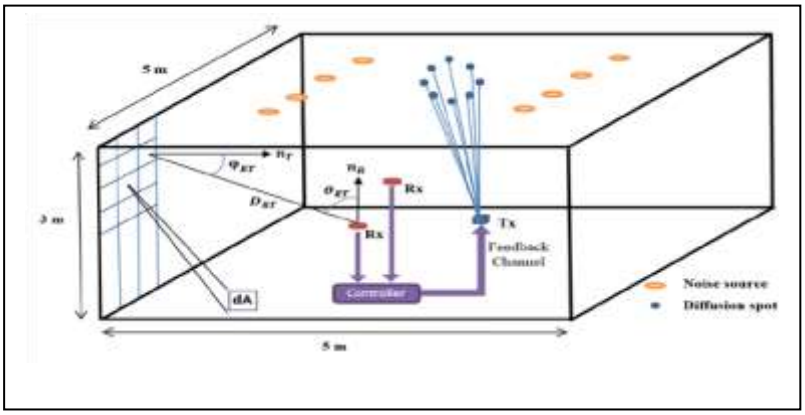

Figure 2.1: Structure of Indoor Owc System(Eltokhey, 2019)

may result in loss of pulse amplitude and inter symbol interference as shown above in Fig. 2.1. Hence, there is a maximum transmission speed which depends on the room size and reflection coefficients inside the room (Chen *et al.* 2020). It was shown that at higher degrees angle of FOV, the receiver will detect all the signals which fall on the receiver area (Wong D *et al*, 2005).

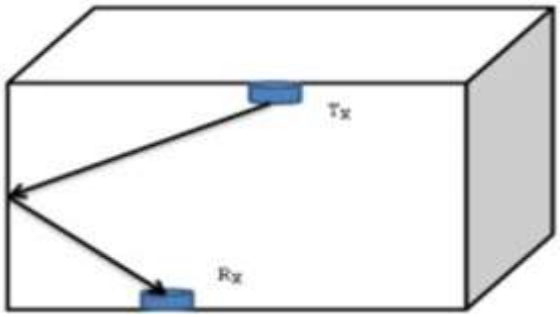

Figure 2.2: Diffusion channel

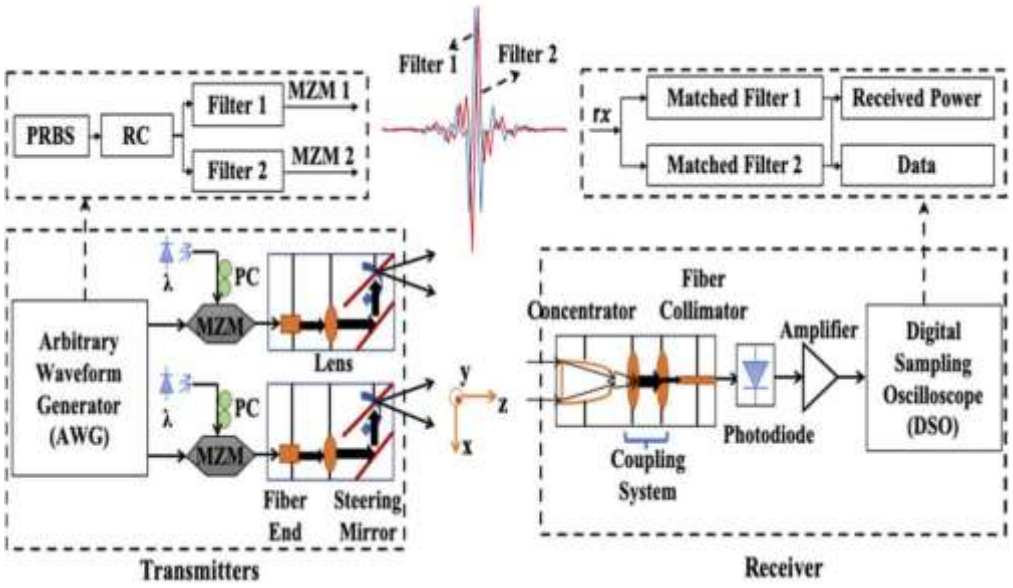

Figure2.3: Indoor optical wireless communication system with continuous and simultaneous positioning

2.1 Types of OWC Systems

a. Infrared Light Communication with wavelength range; 1mm- 750nm.

b. Visible Light Communication with wavelength range; 780nm-380nm.

c. Ultraviolet Light Communication with wavelength range; 10nm-400nm.

2.1.1 Infrared light communication (IRC) :

which appears to be very attractive way to complement radio frequency communication systems, it has found many areas of usage, almost in every home (Zadobrischi *et al*. 2019) (Soltani Mohammed 2019), an Infrared Light communication is one of the most promising candidates for high−speed in−house(Stassen and Colak 2020). This supports speed up to 115Kbps but the limiting factor is distance between the two terminals should be low, and a line of sight (LOS) is always needed. Infrared communications are very successful in the field of direct communication between buildings, although very high rates up to hundreds of Mb/s can be achieved(Zou *et al*, 2016).

The achieved high rates are also due to more relaxed eye safety limits in IR compared to visible wavelengths. Relatively high power is allowed because the retina is less vulnerable with IR light(Chun *et al.* 2019).

2.1.2 Visible light communication (VLC) Systems

Visible Light Communication (VLC) technology using White LEDs is gaining attention in academia and industry, driven by progress in white LED (WLED) technology for solid state lighting and the potential of simultaneously using such LEDs for wireless data transmission. The VLC system with an imaging receiver provides low delay spread, it also provides good SNR at high data rates compared to the other systems (Alsulami *et al.* 2018). The oscillation in delay spread is due to the proximity (or otherwise) from the transmitters (light sources in VLC) as the receiver moves along the *y* axis. The oscillations in the SNR are due to similar effects and can be more significant in infrared systems where the room lighting can act as a noise source. The use of optimum receiver element selection or receiver element signal combining techniques in ADR (Arfaoui *et al*. 2020) and imaging receivers (Zou et al, 2016), can result in more uniform SNR in the room where the best receiver element that avoids noise and/or interference for example is selected (Abdelrahman and Abdulwahab 2019). In general, the LOS link configurations either direct-LOS or Non direct-LOS and diffused spots in commonly used for VLC. However, the link can provide uniform optical radiation pattern across the room and make the system mobile (movement or rotation of the receiver units is realistic) (Abdelrahman and Abdulwahab 2019).

2.1.3 Ultraviolet

The responsivity of the photo detector at ultraviolet range is far lower than that of visible range, high power UV transmitters which can be easily modulated are under investigation. These factors make it is hard to realize a high-data-rate diffuse-LOS or NLOS UV communication links *(Haas et al.2020).*

On these grounds, the VLC technology is considered to have high potential in the 5G / 6G context. In most cases, the VLC technology is considered as a complement for the RF based solution. In this scenario, VLC can be used for high speed downlink, whereas RF can be used for the uplink. Thus, VLC can contribute to RF network offloading and it can enable higher data rates (Zadobrischi *et al.* 2019); (Amsters *et al*, 2019).

2.1.4 Links configurations in OWC

There are two criteria to classify OWC links:

(a) The level of directionality of the receiver and the transmitter and,

(b) If there is a direct path between the receiver and the transmitter. These classifications are based on the radiation pattern of the transmitter and field of view (FOV) of the receiver (Amsters *et al*, 2019).

2.1.5.1 Line of sight links

Provide a direct path between the transmitter and the receiver which minimizes multipath dispersion and enhances the power efficiency of the communication system. However, LOS links suffer from shadowing.

2.1.5.2 Non-line of sight links

Rely on reflections from the walls, ceiling and other objects. They offer robust links and protection against shadowing but are severely affected by multipath dispersion, which results in ISI and pulse spread. Both LOS and NLOS schemes can be classified into directed, hybrid and non-directed. The NLOS non-directed scenario is considered to be the most desirable method for indoor systems from the point of view of mobility, however it suffers dispersion which can limit the achievable data rate and is also limited by the low power collected.

2.1.5.3 Diffuse system

Is the conventional diffuse system (CDS), it employs a wide FOV receiver and a transmitter with wide radiation pattern. The transmitter and receiver point towards the ceiling and the received signal reaches the receiver through multiple reflections. The CDS impairments can be reduced by using specific receivers, such as the triangular pyramidal fly-eye diversity receiver which uses an optimum value of the FOV to mitigate ISI in indoor OWC systems (Alsulami *et al.* 2018).

2.1.5.4 Non-Los diffused link

It is also called Line Strip Multi beam System (LSMS) links/ NLOS (hybrid link. The NLOS hybrid system where the transmitter faces up produces a number of spots on the ceiling by dynamically controlling the powers of individual diffusion spots, a consistent power distribution, with negligible impact to bandwidth and rms delay spread, can be established in indoor OWC systems using this link (Chen *et al.* 2020); (Alsulami *et al.* 2018).

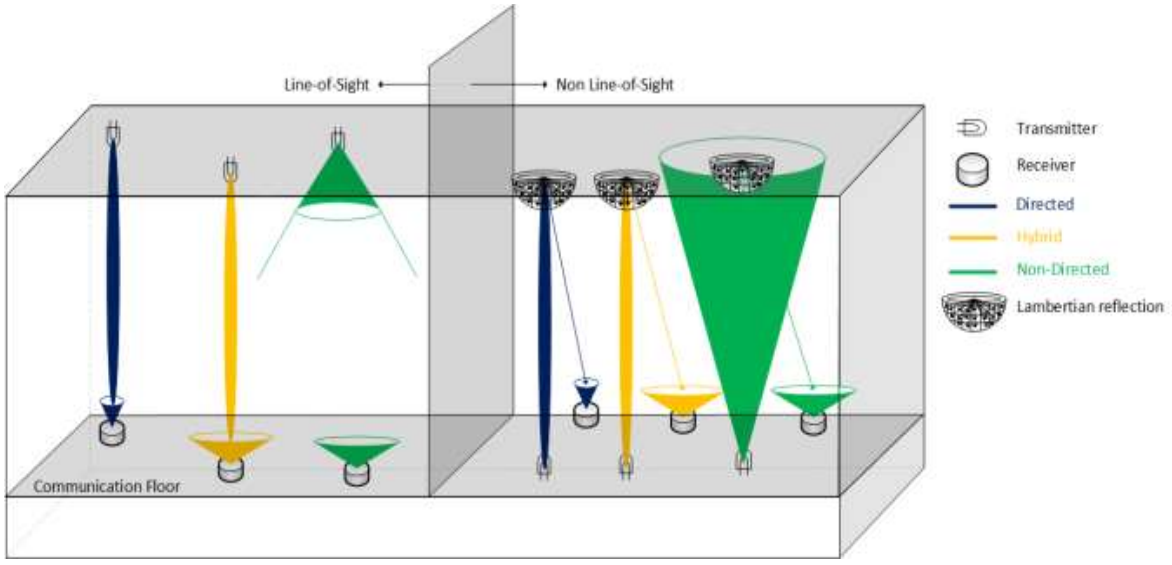

Figure 2.4: Optical wireless link classification

2.3 Advantages of Optical Wireless Communication Systems

The Optical Wireless Communication technology is based on a preexisting lighting network and on low-cost components. Hence, the cost of the implementation can be significantly reduced. So, instead of installing a high number of complex communication systems, the existing lighting network could be enhanced with multi-Mb/s data communication abilities. In addition to the above, The ability to provide very high data rates is a significant benefit of optical wireless communication systems (Alsulami *et al*. 2020). In indoor applications, VLC has received increasing attention for more than two decades, in particular, for providing high-speed wireless connectivity, which is also usually referred to as Li-Fi. This has been driven by some specific features of the VLC technology (with respect to the general OWC), including the use of light-emitting-diode (LED)- based luminaires for data transmission, and inherent security due to light confinement in most indoor scenarios. Among current research topics on VLC networks, we can mention addressing multiple-access requirements and user mobility. In particular, special attention

has been devoted to the design of efficient multi-cell architectures in order to ensure network coverage and user mobility in relatively large indoor spaces.

OWC provide an intrinsic spatial isolation of the neighboring cells. Furthermore, when considering that a room can have more than a LED light, in most cases each work space has its own light source shown fig. 1.6 below, by this action, and the size of a cell is further reduced (Rahman *et al*, 2019).

On these notes, the LED technology is consider to have high potential in the 5G / 6G context, hence VLC technology is consider as a complement for the RF based solution. In the above situation, VLC can be used for high speed downlink, whereas RF can be used for the uplink to complement each other. Thus, VLC can contribute to RF network offloading and it can enable higher data rates (Zadobrischi *et al.* 2019).

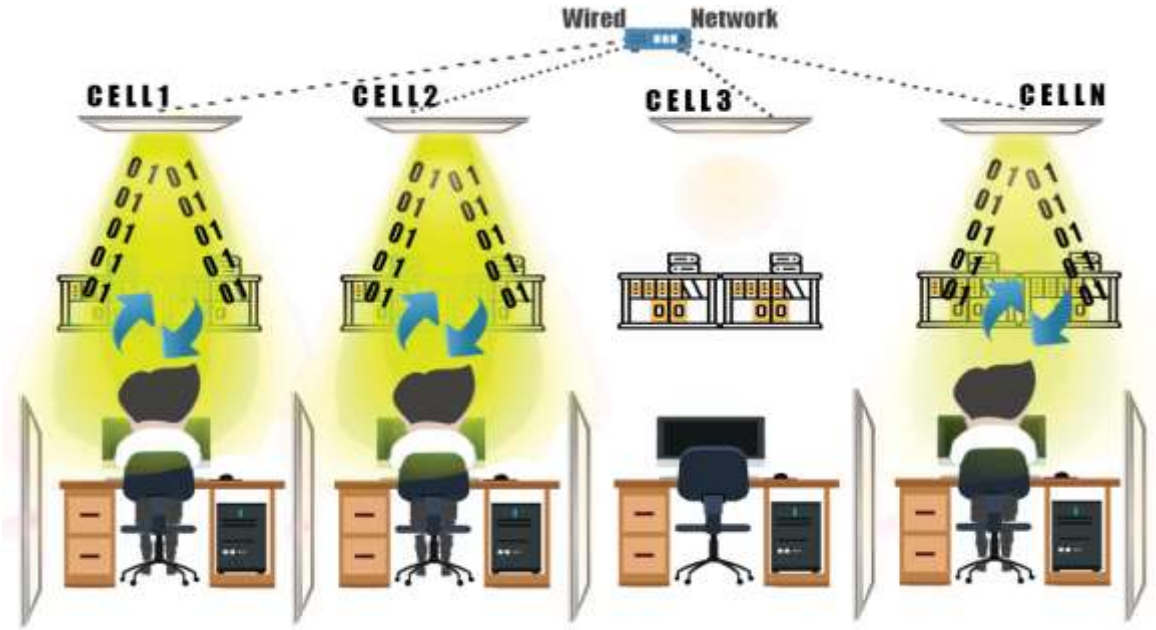

Figure 2.5 Practical use of Light Emitting Diode in Indoor Environment.

High Data Rate Communications was Provided using the lighting system as it is shown above Zadobrischi *et al*. (2019).

Similarly, in addition to an extended spectrum, VLC has as main advantage the fact that it is based on the wide distribution of the lighting sources. Thus, any LED-based light source can be easily transformed in a data transmitting device, that uses the visible light to provide illumination and data transfer simultaneously(Chun *et al.* 2019). In this context, the IEEE 802.15.7 standard imposes that the data transfer function has no effect on the lighting function. Hence, the standard specifies that the power of the emitted light must be adjustable to the user's needs of optical wireless communication that used visible light to transmit data, it is used widely in indoor communications systems and besides its low cost due to the used of LED as transmitter and photodiode as receiver, this technology does not cause any side effects on the human eyes. However, with the continuous dramatic growth in data traffic, researchers from both industry and academia are trying to explore new network architectures, new transmission techniques and new spectra to meet these demands (Arfaoui *et al.* 2020).

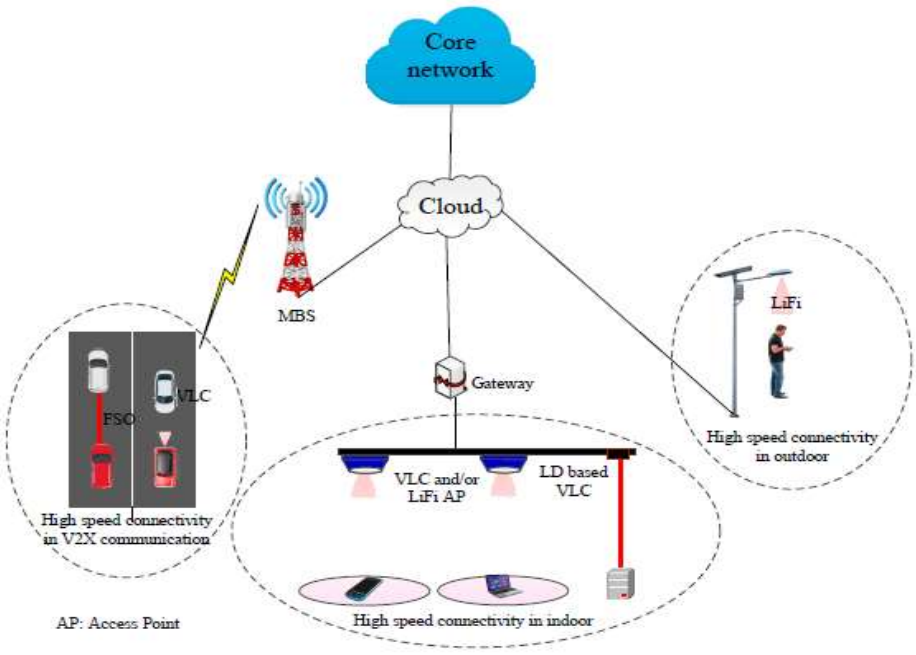

Figure 2.6 High-speed connectivity using different OWC Technologies.

2.4 Challenges of Optical Wireless Communication Systems

i. **Infrared Light Communication (IRC) Systems:** One of the limiting factor of IRC is distance between the two terminals must be very short, and a line of sight (LOS) must be establish between the terminals. Another disadvantage is that; it is unsustainable in heavy weather conditions such a snowfall or fog. The link cannot be sustained then, due to increased path loss between terminals. In indoor environments, IR signals reach the receiver along the Line of Sight (LoS) path, but also along other MPs due to signal reflections on surfaces in the environment.

ii. **Visible Light Communication:** The total data rate of the VLC link in the multi-channel reflection environment depends on the delay of the propagation path. Furthermore, total power gain can be increased by narrowing the angle of FOV of the LED. In Diffused Spots Link OWC system each of the components reaches the receiver with a different power strength and phase than signals that have traveled along the LoS (De-la-llana-calvo *and Lazaro-Galilea* 2019). Another challenge for the high-speed VLC is light dimming which affects the link performance. There are two main approaches for dimming: (i) amplitude reduction and (ii) pulse width modulation (PWM). In the first approach increasing the link power budget could help to maintain the link target performance. Consequently, data transmission combined with PWM dimming, is required to operate in burst mode and to coordinate with the duty cycle of dimming pulses.

According to (Stassen and Colak 2020), there is need for Optimization of Multi−Spot Diffusing Configuration due to the aforementioned issues.

This research focused on the problems the previous authors tried to solve, tools and methodologies used and results they achieved/outcome of their study. In this work; optimization of diffuse spots' parameters in indoor optical wireless communications (OWC) system was proposed by using the particle swarm optimization (PSO) algorithm, Jaya algorithm and also making comparison between the two (2) algorithms. Simultaneous optimization of the diffusion spots' locations and intensities, we propose an improvement in the signal-to noise-ratio (SNR) and minimal the delay spread at the receivers, while considering both the background noise and the multipath dispersion.

Table 2.1: Comparison between RF System/ OW System

Property	**Radio Frequency System**	**Optical Wireless System**
Band width regulated	Yes	No
Security	Low	High
RF Interference	Yes	No
Passes through walls	Yes	No
Technology Cost	High	Low
Beam directivity	Low	Medium
Availability of Band Width	Low	Very High
Transmitted Power	Restricted(Interference)	Restricted (Eye, Skin Safety& Interference)
Noise sources	Other users and system	Sunlight and Ambient light
Power Consumption	Medium	Relatively low

2.5 General Review of Data Rate in Both Rf and Optical Wireless Communication Systems.

The upcoming fifth- and sixth-generation (5G and 6G, respectively) communication systems are expected to deal with enormous advances compared to the existing fourth-generation communication system *(Zou et al. 2017).*

The few important and common issues related to the service quality of 5G and 6G communication systems are high capacity, massive connectivity, low latency, high security, low-energy consumption, high quality of experience, and reliable connectivity. 6G communication will provide several-fold improved performances compared to the 5G communication regarding these issues. Optical wireless communication (OWC), along with many other wireless technologies, is a promising candidate for serving the demands of 5G and 6G communication systems. In this paper (Chowdhury and Hasan 2019) obviously presents the application of OWC technologies, such as visible light communication and other optical communication technologies as an effective solution for successful deployment of 5G/6G.

Vision and Key Features for Future Networks, the missing units from LTE and 5G that must integrate, research communities have set out research modalities on the formulation, along with AI and deep neural networks (DNNs), are revolutionizing technology that definition, design, and identification of important core-enabling technologies driving the initiation toward a “beyond 5G” or 6G system.

The research for the High Data Rate by *(Chataut et al, 2020)* The need for an efficient cellular spectrum that can accommodate the tremendous surge in wireless data traffic is imminent, they suggested that, Massive MIMO wireless access technology is the answer to this global demand. Massive MIMO technology groups together antennas at both

transmitter and the receiver to provide high spectral and energy efficiency using relatively simple processing techniques.

Given the worldwide need for an efficient spectrum, a limited amount of research has been conducted on massive MIMO technology. According to the authors, several open research challenges are still on the way of this emerging wireless access technology (OWC).

The advent of THz waves into a mobile network portfolio could provide solutions for those applications where 5G technology failed to meet the high data rate requirement or ultra-reliable low latency regimes, Plasmon-based THz link components present a promising solution for THz communications due to their extremely small size and ability to operate at ultra-high data rates, they could be perfectly combined with photonic technology *(Le et al, 2010)* and with dielectric wave guiding relatively long interconnect distances and drives new research opportunities in various areas, including 6G communications and IoTs (Alsharif *et al.* 2020).

Operational intelligence (OI): This technology allocates resources efficiently to achieve satisfactory network-operations instead of involving traditional methods, using multi objective optimizations that can work in the highly complex and dynamic nature of 6G owing to its heterogeneity, density, and scalability. Such optimizations that measure prioritizing multi-objective performance are typically NP hard problems and are difficult to measure in real time communication/data service providers, as expected, this aspect will become a soft spot in the human-centric 6G technology and might produce a calamitous outcome without appropriate countermeasures. machine-type communications (MTCs) and vertical-specific wireless network results for 6G are examined in the work suggests that 6G could hasten the development of the first-ever barrier-breaking standard and offer an integrated solution permitting effortless connectivity of all needs in vertical industries.

The challenges regarding communications stem from five key components: provision of network security and data privacy enforcement, attainment of a cost-effective approach towards rapid network deployment and expansion with an emphasis on remote and stand-alone areas, reduction in the price of mobile communications utilization, approaches to extend mobile equipment battery life longevity, and attainment of a higher data rate buoyed with end-to-end, ultra-reliable low latency regime. The balance between privacy and intelligence would be significant in 6G networks, as they are humanoid networks, Customization attracts increased attention, and Intelligence versus exorbitant routines and Intelligence versus sub-routines are needed for AI algorithms and smart nodes such routines and sub-routines should be specified in the most fundamental procedures of networks. High intelligence comes at a cost in terms of network complexity and could translate to higher network operators and gadget producer budgets, which would lead to a higher device cost for consumers and negate the dream of providing affordable gadgets.

Secrecy and privacy are guaranteed, consumers are permitted to exchange the available anonymized data for a reduced data price, Analogous to this scheme is the smart grid concept, through which electricity consumers' trade their own-produced electricity with electricity power firms, and which would be borrowed by 6G communication networks *(Wu et al, 2021*).

Achieving end-to-end, attack-proof wireless data communication requires many spectrum bandwidth preventive measures which results in a reduction in the available spectrum data available for data transmission (Sindri *et al.* 2020).

Finding an acceptable scheme to address the security and spectral efficiency concerns of wireless communications would entail complex computations and the environmental advantages obtained via ubiquitous intelligent surfaces would be crucial in reducing the

spectrum-energy tradeoff by responding to the ever-changing radio propagation conditions. The current transceiver structure is considered as one of the main challenges in utilizing the THz band, so sophisticated signal processing is required to handle the massive propagation loss at THz band frequencies. Other parameters, such as the high power, high sensitivity, and level of noise figure must be handled. In THz frequency bands, utilizing silicon germanium-, gallium nitride-, gallium arsenide-, and indium phosphide-based technologies is highly possible, but designers must consider the limited power gains in mobile networks The conventional complementary metal oxide semiconductor technologies and the recently introduced nano-materials, such as graphere can be utilized for novel transceiver architectures for THz-enabled equipment The massive data rate in the THz band and available bandwidth can be exploited in fast communication networks *(Zhang et al, 2020)*. Small cell networks tend to involve attraction reflecting user-centric hotspot areas, whereas repulsion is observed at the macro cell level to represent rural and urban deployments this distinction will be more emphatic in very small cell environments.

In a paper titled; An End-To-End LwM2M-Based Communication Architecture for Multimodal NB-IoT/BLE Devices by (Karaagac *et al.* 2020) proposed architecture for multimodal NB-IoT/BLE devices It consists of the end device, the network and the backend server looking at the right side of the architecture, it is clear that in case IoT devices are allowed to use different communication technologies and modes, there should be an entity that will merge the traffic coming from both technologies/networks as well as decide which technology to use in downlink.

In another paper, (Borcoci 2020) considered safety of the transferred data and not speed, hence need to improve on the data rate, Two level hierarchical SDN control Tenant controller (TC) and infrastructure SDN controller, each logically placed in different

administrative domains. Tenant Controller (it can be deployed as a VNF itself) dynamically configures and chains VNFs (graphs) to realize NSs in the tenant domain only controls the SW apps. of the VNFs for configuration and chaining purposes, but not their underlying NFVI resources offers a set of dedicated northbound I/Fs that allows slice's clients (and thus tenant's clients) to interact with the slice Infrastructure Controller, manages and controls the NFVI network resources (placed in a NFVI-PoP or a WAN) to set up the connectivity for communicating the tenant VNFs in the infrastructure domain (i.e., among the virtualization containers that host the tenant VNFs' SW applications) under VIM control. Security Each admin domain may have its own security domain e.g. one security domain for each InP, one security domain for each tenant, and one (or more) security domain(s) for each slice clients may come from different organizations the definition of separate security domains in the slice is required to preserve security and privacy isolation between clients the abstraction and isolation that the TC enables with its northbound interfaces helps to accomplish this security level.

In (Ahmad *et al.* 2020) A wide-band and tunable Q-switched erbium-doped fiber (EDF) laser operating at 1560.5 nm with a tungsten ditelluride (WTe_2) saturable absorber (SA) is demonstrated. The semi-metallic nature of WTe_2 as well as its small band gap and excellent nonlinear optical properties make it an excellent SA material. The laser cavity uses an 89.5 cm long EDF, pumped by a 980 nm laser diode as the linear gain while the WTe2 based SA generates the pulsed output. The WTe2 based SA has a modulation depth, non-saturable loss and saturation intensity of about 21.4%, 78.6%, and 0.35 kW/cm2 respectively. Stable pulses with a maximum repetition rate of 55.56 kHz, narrowest pulse width of 1.77 μs and highest pulse energy of 18.09 nJ are obtained at the maximum pump power of 244.5 mW.

A 56 nm tuning range is obtained in the laser cavity, and the output is observed having a signal to noise ratio (SNR) of 48.5 dB.

Other reviews of VLC systems application is underwater sensor, In this paper titled " End-to-End Performance Analysis of Underwater Optical Wireless Relaying and Routing Techniques Under Location Uncertainty, *(Celik et al. 2020)*. The recent demand on high quality of service communications for commercial, scientific and military applications of underwater exploration necessitates a high data rate, low latency, and long-range underwater networking solutions, fulfilling these demands is a formidable challenge for most of the electromagnetic frequencies due to the highly attenuating aquatic medium. The estimated node locations may not refer to actual node positions either because of the localization errors or the random movements caused by the hostile underwater environment these have negative impacts on the link reliability and performance as a result of the poor PAT efficiency. According to them, it was of utmost importance to develop robust relaying and routing techniques which manipulate range-beam-width tradeoff by means of adaptive optics, which was main focus of this paper. They model the displacement of the actual locations from the estimates, consider an uncertainty disk whose radius is a design parameter that depends on the localization accuracy and/or mobility of nodes, assumed nodes are equipped with adaptive optics, robust UOWC links are provisioned by deriving the divergence angles for scenarios with and without a PAT mechanism. The authors investigated and compared two prominent relaying techniques; decode & forward (DF) and optical amplify & forward (AF), each of which is analyzed for important E2E performance metrics for both relaying methods, closed form expressions were derived for various performance metrics, e.g., E2E-Rate, E2E bit error rate (BER), transmission power, amplifier gain, etc. It concludes that, LiPaR can provide a superior performance compared

to centralized schemes without a PAT mechanism, this system model can reach nearby nodes whereas a narrow divergence angle is able to reach distant destinations, manipulation of this tradeoff has significant impacts on several performance metrics such as the degree of connectivity, distance progress for the hop, routing efficiency, and E2E performance, a narrow divergence angle can deliver a desirable performance over long distances, which requires precise and agile PAT mechanisms to keep the transceivers aligned over long ranges.

2.6 Review of Data Rate in Optical Wireless Communication (Diffuse Spots Link Only)

The diffuse spots link configuration of optical wireless communications system where the transmitter (i.e. visible light communication) and multiple receivers / an angle diversity receiver (photo-detector) are not in fixed line of sights.

A comparison was made between different optimization scenarios, to illustrate the effect of varying the parameters that are being optimized.

A quasi-diffuse link based on multi spot diffusing (MSD), was first proposed by Yun and Kavehrad (1993), the link utilizes multiple narrow beam transmitters and an angle diversity receiver (ADR); that is, several narrow FOV detectors in Indoor optical wireless systems and NLOS configuration employed, 10s of Kb/s speed was achieved.

According to (Zhang *et al.* 2020) It was assumed that the light source is a near-lambertian light source and the reflective surface is a standard lambertian surface.

In the LED industry, people use the half power angle $\theta 1/2$ as a measure of the angle of illumination. The half power angle $\theta 1/2$ is defined as the angle between the axial direction and the direction in which the luminous intensity is half with the axial direction, the half power angle $\theta 1/2$ of the standard Lambertian source is 60^0. *In practical applications, the*

LED half power angle $\theta_{1/2}$ is often not equal to 60^0. Such an LED is called a near-Lambertian light source, and the luminous intensity function is expressed as:

$$I_\theta = I_o \cos\theta \qquad 2.2$$

where m is the order of the Lambertian source. Combined with the definition of the half power angle So, we know that the order of the Lambertian source m and the half power angle 1/2 correspond to each other. The order of the Lambertian source m can be obtained by the half power angle 1/2, and the normalized luminous intensity distribution function.

$$m = \frac{\ln 2}{\ln(\cos\theta_{\frac{1}{2}})} \qquad 2.3$$

(Khalighi *and Ghassemlooy* 2021): A special case of VLC is when the camera of a smart device is used as the detector, commonly known as optical camera communications (OCC), where data transmission is based on spatial and temporal variations of light intensity. OCC can be regarded as one of enabling technologies for IoT connectivity in future smart environments (figure 5) as in the above illustration. The main challenges here include increasing the data rate, which is mainly limited by the camera exposure time and the frame rate.

The proposed design in (Abdelrahman and Abdulwahab 2019) which presented VLC system using four LEDs placed on the room corners in rectangular configuration. The results of the measured SNR in his model was 82.2 ~ 87.2. The indoor communication environment is an 8m×8m room with a height of 3 m. The transmitting LEDs are placed on the ceiling, and the receiving device is placed on a receiving plane, number of transmitters LEDS is four, which is distributed in circular deployment, the paper suggested three different deployments to be studied which were defined but, delay spread was not considered. User mobility and link blockage are the other important aspects of indoor

system networks, these factors and in particular, random device orientation can highly affect the system performance and seamless connectivity which also affect the received signal-to-noise ratio (SNR) and as a result the throughput remarkably in millimeter wave *(Soltani Mohmmed 2019).*

In a related development; Receiver alignment dependence of a GA controlled optical wireless transmitter A System Model was define based on system environment to be an arbitrary indoor rectangular room for which the majority of surfaces exhibit a fully diffuse reflection characteristic that can be described by Lambert's reflection model From a receiver point of view, if both LEDs and the reflected radiation from a 2-D VCSEL/RCLED array appear as sources exhibiting a lambertian radiation intensity pattern, this model simplification, is such that each of the I diffusion spots on the ceiling will be considered independent sources Si. The only error induced with this assumption is a delay and propagation loss between the emitting element of a 2-D VCSEL/RCLED array and the diffusion spot position. The OWC radiation incident upon a receiver Rj will be the result of the radiation emitted from a source Si that has propagated directly through an unobstructed LOS path, and/or from the radiation that has undergone a finite number, k, reflections off the surfaces within the environment. It is known that, for an intensity modulation, direct detection (IM/DD) channel, where the movement of transmitters, receivers or objects in the room is slow compared to the bit rate of the system, no multipath fading occurs, and, as such, can be deemed an LTI channel. Channel Model for a non-directed OWC channel employing IM/DD, a source Si, which emits an instantaneous optical power Xi(t), will produce a instantaneous photocurrent Yij(t) at receiver Rj with photodiode responsivity rj, in the presence of an additive, white Gaussian shot noise Nj(t), and can be modelled as the linear baseband system, such that, by incorporation all of the receivers will attain the same

or very similar photocurrents, by normalizing the I scaling factors, the equality result is independent of receiver power magnitude, and secondly for different environments, they can adjust for example, the pulse characteristic, in order to increase or decrease the received power to make the power distributions equal. The RMS delay spread can be found from the original impulse response. Due to the stochastic nature of the GA, for each simulation the results were inevitably slightly different, meaning that, to allow presentation of results that are both representative of the GAs performance, we conducted each simulation 30 times, such that each performance value presented within section 5 of this work is the average after the 30 retrials, the result of receiver alignment is purely based on one receiver with a given FOV at one location in one environment. Taking into account the presence of many receivers that can be independently orientated, the problems an OW system designer faces become apparent.

The authors, demonstrated the approach of using a GA controlled MSD transmitter, capable of optimizing the received power distribution in multiple environments with user movement and alignment variability, relationships have been drawn between the effectiveness of GA channel optimization and the receivers FOV, and statistical alignment probabilities, user movement has been shown to perturb the channel by up to 10%, which can be reduced to as little as 2.5% using the GA, the optimization has been achieved with negligible impact on the bandwidth and RMS delay spread, and overall the method has shown the possibility of providing a highly adaptable method of overcoming channel variability with a solution that reduces receiver complexity for deployment application and the two algorithms presented have been shown capable of reducing the power deviation by up to 26% in an empty room, and maintaining to be within 7% of this optimized case the power distribution when the user perturbs the channel through movement..

Full-duplex high-speed indoor optical wireless communication system based on a micro-LED and VCSEL array Visible light communication (VLC) was proposed by (Wei *et al.* 2021), one of the typical optical wireless communication (OWC) technologies, loads digital baseband signals into illumination light emitting diodes (LEDs) for data communication through high-speed intensity modulation In a typical indoor environment, the downlink needs to be high-capacity to support larger download traffic and multiple users which requires the downlink to use high electrical-to-optical (E-O) bandwidth illumination device such as micro-size LED and complex multi-carrier modulation techniques represented by quadrature amplitude modulation orthogonal frequency division multiplexing (QAM-OFDM). The data rate of VLC has reached 7.91 Gbps by using a gallium nitride (GaN) violet micro-LED with E-O bandwidth of 655 MHz, but the system is limited by a very short communication distance of 27.5 cm The data rate reached 2 Gbps employing quantum dot (QD) blue micro-LED with simple non-return-to-zero on-off keying (NRZ-OOK), indoor environment with 5 m × 5 m × 3 m size and implement the measurement for the downlink (a blue QD micro-LED-based) and a near infrared VCSEL

array-based lens-free uplink, respectively. (Rahman, Bakaul, and Parthiban 2018): This paper analysed the impact of the field of view of the LEDs and reflection paths on the performance of a visible light communication system, when FOV was varied from 35° to 75°, the total received power varied by around 6dBm. The reflections can degrade BER by an order of magnitude around 10-5, this means the selection of LEDs' position inside a room and their FOV is important to increase the data rate and illumination quality so this analysis would help in estimating necessary parameters for the VLC model and its applications for the high speed communication link.

In this paper (De-la-llana-calvo *et al.* 2019), the authors proposed a model to characterize Infrared (IR) signal reflections on any kind of surface, a simplified model based on only two reflection components, together with a method for determining the model parameters based on 12 empirical measurements that are easily performed in the real environment where the IR-LPS is being applied. Their experimental results show that the model provides a comprehensive solution to the real behavior of IR MP, yielding small errors when comparing real and modeled data (the mean error ranges from 1% to 4% depending on the environment surface materials). Other state-of-the-art methods yielded mean errors ranging from 15% to 40% in test measurements. The values for the seven model parameters are obtained by data fitting in the Equation using experimental measurements. The error depend on both the number of measurements chosen and the angle where these measurements were obtained so also an acceptable error between the model and the real system was adopted, using genetic algorithms to determine how many measurements took place at which angles of incidence and reception, analyzing all available measurements to minimize both the number of points used in the function fitting and the error between the model adjusted with these points for all available experimental measurements, the system would be to complex to implement. In another work; Data Centre optical wireless downlink with WDM and multi-access point support (Alsulami *et al.* 2020).

The amount of personal computers and individual digital assistants for indoor use are rapidly growing in offices, manufacturing floors, shopping areas and warehouses, the bandwidth of wireless infrared systems is limited due to inter-symbol interference produced by the multipath dispersion of the optical channel PPM offers greater average power efficiency but increases system complexity compared to On-Off Keying (OOK) since both slot- and symbol-level synchronization are required in the receiver, and are critical to

system performance. In FH-Code-Division multiple Access (CDMA), the information bits modulate a group of frequencies, which are hopping according to pseudo random numbers. Point-to-Point or Directed Beam Infrared (DBIR) local area networks (LANs): In recent years, the application of point-to-point or DBIR radiation to wireless information networking has been extensively investigated and some products using this technology are in the market .This paper has provided a review of the main issues associated with the physical layer of a wireless optical communications system. Adopted dimension was (length × width × height) 8 m × 8 m × 3 m and A data rate of 8.5 Gbps can be achieved for downlink communication for each row at the same time by using the ImR, while the ADR provides varied data rates between 1.5Gbps and 7 Gbps. The ImR provides better results compared to the ADR in terms of the supported data rate, there is effect of shadowing and blockage of signal in the system.

This research paper: Indoor Optical wireless communication system with continuous & simultaneous positioning (Wang *et al.* 2021), the wireless communication needs to be paused for sending dedicated positioning signals, and this reduces the effective OWC data rate and limits the overall communication capacity, especially when the number of transmitters is large Since both positioning and wireless communication functions share the same system, the user positioning can only be obtained at discrete positioning time slots and continuous positioning cannot be provided. The concept has been extended with the use of orthogonal-frequency division-multiplexing (OFDM) for optical wireless communication, where a dedicated OFDM sub-carrier is allocated to each transmitter for the positioning purpose This method requires dedicated RF carriers or subcarriers to carry the positioning signals, and this reduces the useable bandwidth of each transmitter, and affects the communication data rate and system capacity (Wu *et al* 2011).

Results show that similar positioning accuracy can be achieved without interruption to the wireless data communication, RSS-based indoor OWC positioning system they assumed that repetition coding (RC) is applied to the transmitters for wireless communications, since compared with other transmitter diversity scheme such as space-time-block coding (STBC), the RC scheme has shown to be highly effective in indoor OWC systems in providing better robustness, increasing the data rate, or extending the signal coverage area. Assuming that the optical signal to be transmitted by OWC transmitters is TX, which is a matrix with Mtx × 1 dimension, and the channel gain is H, which has a dimension of Mtx × Mrx, the detected electrical signal RX can be expressed as: RX = R ⊙ (TXT H)T + N Since the aperture size and the optical beam footprint are pre-known, when there are more than two transmitters available, the positioning of user can be obtained by monitoring the RSS and estimating the corresponding channel gain information from each transmitter, it is challenging to apply these positioning schemes together with RC, as this affects the OWC robustness and coverage area.. Filter-enhanced RSS-based indoor OWC positioning system; after applying RC to the transmitted data and modulating them onto optical carriers, rather than sending the modulated optical signals out directly for data communication or positioning, a dedicated waveform shaping filter is allocated to each OWC transmitter. Given this property of the filters, the output of the matched filter k of receiver j, from the channel gain estimation process shown, it can be seen that the noise existing in the received optical signal affects the channel gain estimation accuracy, and it limits the positioning accuracy that can be achieved.

The proposed indoor OWC positioning system employs spatial waveform shaping filters, the RSS information can be obtained directly from the wireless communication signals to

realize the positioning function. Method used; minimal interruption to wireless communications via Long codes required dedicated codes for transmitters, the FDM-based method has the fundamental limitation of reduced data rate per transmitter compared with the single transmitter case, as only a fraction of available frequency can be used. With the use of spatial waveform shaping filters, multiple transmitters can use the same full frequency band, and the data rate per transmitter is the same as the single transmitter case. This advantage of proposed scheme becomes more significant when the number of transmitters increases, since the data rate per transmitter further reduces in the FDM-based scheme due to the sharing of the same frequency band by more transmitters.

To demonstrate the proposed filter-enhanced indoor OWC positioning system, they considered the simple case with two near-infrared transmitters. The RC signals were generated using an arbitrary waveform generator (AWG) with 223–1 PRBS data, and they were modulated onto the optical carriers generated by lasers using two Mach-Zehnder modulators (MZMs).

The impulse responses of the two orthogonal waveform shaping filters were shown in the inset, the impact of noise becomes larger and the positioning accuracy decreases this trend is reflected in the measured BER performance, where compared with the results shown the BER was better at locations close to the signal beam centers and worse at locations close to the beam edges. It can be seen from the results that the positioning and wireless communication functions can always be achieved simultaneously, demonstrating the capability of proposed filter-enhanced indoor OWC positioning system, Filter-enhanced RSS-based indoor VLC positioning system

In the previous analysis and demonstrations, the near-infrared indoor OWC system using the near-infrared wavelength and laser transmitters was considered, by considering an

indoor environment with Mtx LED transmitters. Considering the LOS link, the wireless channel gain from LED transmitter i to the receiver j and when more than three transmitters are available, the positioning function can be realized via trilateration.

Simulated results shows the feasibility of proposed filter-enhanced VLC positioning system via simulations .It can be seen that the average positioning accuracy achieved in the simulation using the proposed filter-enhanced method is about 6.15 cm, and better positioning accuracy is achieved when the receiver is closer to the room center, where a better BER performance is achieved, and this is mainly due to the larger signal power detected. The wireless communication signals from different LED transmitters can always be separated using the proposed filter-enhanced scheme regardless of the location for positioning directly. Both wireless communication and positioning functions can be realized simultaneously. With the proposed filter-enhanced scheme, signals sent from different transmitters can simultaneously be separated at the receiver side after the matched filers. The system data rate or capacity is not affected. So, the authors of (Alresheedi *et al*, 2016) proposed filter-enhanced indoor OWC system that is capable of simultaneous positioning and wireless communication functions was experimentally demonstrated in a near-infrared indoor OWC system with laser transmitters. An average positioning accuracy of 5.41 cm has been achieved, and 2.5 Gb/s wireless data communication has been realized simultaneously. The feasibility of proposed filter-enhanced scheme in VLC systems with LED transmitters has been studied and demonstrated via simulations. Simultaneous wireless communication with 4-PAM format and positioning has been realized with three LED transmitters. The proposed filter-enhanced scheme provides a promising positioning method in indoor OWC systems without affecting the wireless data communication, the Link employed was LOS.

2.7 Review of PSO Algorithm

In a paper titled Optimal power flow using HFPSO (Abdullah *et al.* 2020) HFPSO algorithm were compared with the standard PSO algorithm and other optimization techniques, the results revealed that optimal solution for each considered case could be presented by the HFPSO algorithm, the new suggested idea of the HFPSO technique led to fast finding of a global solution, results showed the effectiveness of HFPSO technique concerning the satisfactory convergence rate and statistical analysis showed that HFPSO algorithm is a robust and reliable. Another paper "Chaotic Jaya Approaches to Solving Electromagnetic Optimization Benchmark Problems" The Jaya optimization algorithm is a simple, fast, robust, and powerful population-based stochastic meta-heuristic that in recent years has been successfully applied in a variety of global optimization problems in various application fields. The essential idea of the Jaya algorithm is that the searching agents try to change their positions toward the best obtained solution by avoiding the worst solution at every generation. Jaya does not require the tuning of its control, this is the main difference between Jaya and any other matlab coded algorithms, except for the maximum number of iterations and population size parameters. However, like other optimization algorithms, Jaya still has the dilemma of an appropriate tradeoff between its exploration and exploitation abilities during the evolution process. To enhance the convergence performance of the standard Jaya algorithm in the continuous domain, chaotic Jaya (CJ) frameworks based on chaotic sequences were propos

Table 2.2: Summary of the review papers

Reference(s)	*Title*	*Improvements*	*Limitations*	*Link/Techniques*	*Comments*
(Zhang *et al.* 2020)	An optimization of the signal to noise ratio distribution ofan indoor visible light communicat ion system based on the conventiona l layout model	The effective area of the optimal layout of channel quality is increased by 0.32% and 6.08%	Compared with the normal layout, the advantages are not very prominent	The classic indoor visible light communication model, a scheme using the parameter Q to determine the optimal layout of channel quality	Considered the first reflected light and based on the conventional layout model. No delay spread. It require DS to meet future wireless communication needs.
(Borcoci 2020)	Advanced managemen t and control in 5G sliced networks	secured network	Only bandwidth 75MHz was considered, not large enough.	ETSI and 3GPP functional architectures for slicing support	Low Speed & high latency
(Wu *et al*. 2012)	Optimizatio n of lambertian order for indoor non-directed optical wireless	High Data rate	No mobility / more shadowing effects	Genetic algorithm for controlling the optical wireless channel	The delay spread (DS) was not considered in the fitness function.

	communication				
(Eltokhey *et al*,2015)	Optimized diffusion spots locations and simultaneous improvement in SNR and delay spread	Optimization of the center of Diffuse Spots' Distribution was Considered.	The Intensities of the Diffuse Spots (Diss) was not considered.	Diffused link/ Hybrid PSO & CFO	The strengths of the optimization algorithms in solving the problem was demonstrated. We shall try different techniques in order to benefit future switching towards real-time intelligent systems.
(Khalighi *et al.* 2021)	VLC as enabling technologies for IoT connectivity in future smart environments.	OWC application Internet of Things (IoT)	Camera exposure time and the frame rate determine the speed.	Scheduling protocol based on time -division contention-free access scheme.	Addressed blocking in VLC networks. It is not cost effective.
(Eltokhey *et al*, 2019)	Optimization of intensities and locations of diffuse spots in indoor optical wireless communicat	Bit Rate: 50 Mbps Bandwidth:70 MHz (Average SNR, & Average Delay Spread respectively) Scenario X: 17.9881dB	The authors developed optimization based on the impulse response, not, considering that the eye safety	Diffuse NLOS/ PSO Algorithm.	Authors showed that there are up to 42% and 23% improvement achieved in the average delay spread and the average SNR, respectively. Also shown was the improvement in the standard deviation of SNR by up to 65% in the presences of the noises &

	ions	1.0270×10-9s Scenario :Y 19.4327dB 0.9528×10-9s.	regulations must be considered. in term real practical systems. Need improvement.		losses.
(Wang *et al.* 2021)	Indoor optical wireless communication system with continuous and simultaneous position	Simultaneous wireless communication with 4-PAM format and positioning achieved.	No Mobility	LOS Link/ Filter enhance Receive Signal Strength(RSS) indoor OWC	2.5Gb/s
(Alsulami *et al.* 2020)	Angle diversity transmitter for high speed data center uplink communications	The ImR provides better results compared to the ADR in terms of the supported data rate.	Increases system complexity, there is effect of shadowing	LOS Link	1.5Gb/s-7Gb/s
(Chowdhury and Hasan 2019)	The role of optical wireless communicat	OWC is an effective solution for successful	Only RF-based wireless or Optical	The coexistence of the RF and OWC networks can effectively	Did consider hybrid of two different spectrums. Obvious advantages of OWC were discussed.

	ion technologies in 5G/6G and IoT solutions: Prospects, directions, and challenges	deployment of 5G/6G and IoT systems.	wireless communication technologies are insufficient in meeting the demand of 5GB and IoT networks.	solve most of the limitations of individual RF-based and OWC systems	
(Wong *et al*, 2020	Neural-network – based root mean delay spread model for ubiquitous indoor internet of things scenarios	Improvement in the average DS and the standard deviation of the received power by optimizing the spot pattern in diffuse OWC. links	The spots' intensities were not considered	A simulated annealing technique. conventional grid-based designs when an FOV of 10°, 20°, 30°, 45° and 90° for the receiver was modeled in Indoor owc.	Obtain equalized bandwidth at bit rate of 54Mbits/s, an FOV of 30° was chosen as it represents a good tradeoff between the performance criteria.
(Komal *et al*, 2021)	A Heuristic Approach for Optical Transceiver Placement to Optimize SNR and Illuminance Uniformitie	SNR/Illuminance uniformities across the coverage area was considered.	Did not consider Bit-Rate and delay spread.	Barry's benchmark ray tracing Algorithm and performance metrics related to illumination and communication were	The case with minimum SNR fluctuations was compared with the conventional technique. The generation of optimized transmitter locations via the proposed Algorithm 1. Then validation was performed.

	s of an Optical Body Area Network	Computed. LOS Link	Analyze how the placement of light-emitting diode (LED) lamps can improve.

CHAPTER THREE

3.0 MATERIALS AND METHOD

This section is focused on the Formulation of a maximization problem from existing Diffuse Spots Link in Indoor Optical Wireless Communications channel characteristics, we considered lambertian reflectors with a reflection coefficient of r, and only the 1st and the 2nd order reflections are considered, For an intensity modulation direct detection (IM/DD) OWC system, the received photocurrent, the delay spread (DS), For on-off keying (OOK) non-return to zero (NRZ) IM/DD OWC, the signal to noise ratio (SNR). The study will also adopt an optimization of intensities and locations of diffuse spots in Indoor OWC systems, the channel is modeled and the optimization algorithm developed can be generalized for almost any indoor diffuse OWC based local area networks (LAN), with randomly placed Transitions and Receivers.

This study implores comparison of jaya optimization algorithm and particle swarm optimization as method to the formulated problems to obtain optimal solution, and evaluations of optimal solutions for intensities and locations of reflections within the room geometrics showing the power distributions and different values of margin of error for the diffusion spots locations. Below are steps taken in the program:

i. The study will insert values of optimal parameters into Visual Basic Program in the macro chips of CTS MWS suit and automated pattern codes are generated based on the design specification of the diffused optical wireless communications link to obtain optimized intensities and locations of the reflected spots patterns and field of view at the receiver. The values from the results of PSO and Jaya are input into program simulator to run it see Appendix A.

ii. The study will also verify the design to be sure it conforms with the specifications after the simulation values are obtained, CST MWS simulation file will be save as .dxf see also, Appendix A.

iii. Simulation results obtained will be compared with the results obtained from (Eltokhey 2019) and equally measure the bit rate from evaluating singnal to noise ratio (SNR) in dB and delay spread (DS) in (%) and also measure bandwidth efficiency see equation 3.11.

Channel impulse response is given as: $h(t;T_F;R_F)=\sum_{i=0}^{n} \mathrm{h}^r(t;T;R)$ 3.0

And, $h^r(t;T;R)=P_s\sum_{i=0}^{ne}\ \frac{L+1}{2\pi}\frac{\cos^L(\phi_{RT})\cos(\theta_{RT})\times\rho A_R\times rect}{D^2RT}(\frac{\theta RT}{FOV_R})\partial(\mathrm{t}-\frac{DRT}{C})$ 3.1

where L is the lambertian order, P_s is the transmitted power. T_F and R_F are the first transmitting and the final receiving points, respectively, and t and the delta function refer to the time of receiving the impulse response component at the Receiver, but after taking into consideration that the unit impulse is radiated at t = 0 (Higgins *and Green* 2008), r is the reflection order of the impulse response, where r = 0 refers to the LOS component, and nis the number of reflecting elements, T is the point acting as a secondary Transmission , which can be a diffusion spot or a Lambertian reflecting surface, R refers to receiving points, which may be a photo detector (PD) or a reflecting surface (Manousiadis and Yoshida 2020).

$h^r(t;T;R)$ is the r^{th} reflection order impulse response, DRT is the distance between the receiving point and the transmitting point, and AR is the photosensitive surface area or the area of a reflecting element, FOVR is the field of view of the PD, which equals 170◦. When the receiving point is a reflecting element, the term which contains FOVR equals 1.

For x ≤ 1, the rect(x) = 1, otherwise is zero. θ_{RT} refers to the angle between DRT and normal to the receiving point, and ϕ_{RT} is the angle between DRT and normal to the transmitting point n_T. c is the speed of light.

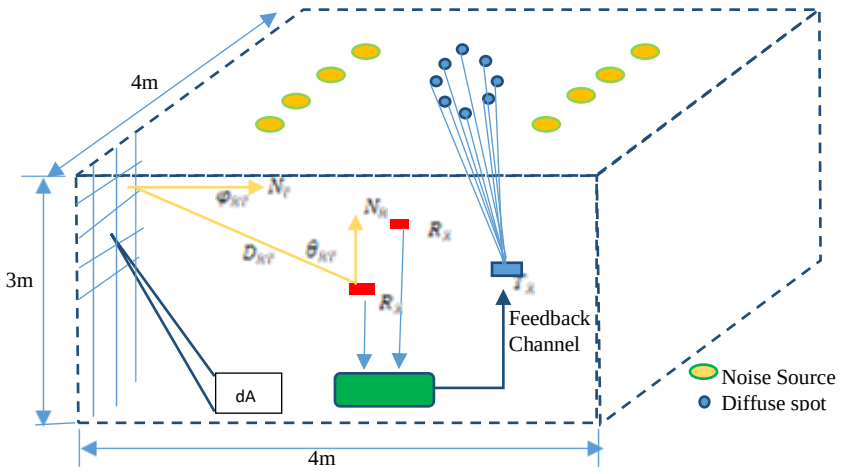

Figure 3.1: Indoor system 3D Design

For an intensity modulation direct detection (IM/DD) OWC System, the received photocurrent is given by:

$$y(t) = RPDx(t) * h(t; T_F; R_F) + n(t) \qquad 3.2$$

Where RPD refers to the responsivity of the Photodetector, x(t) is the transmitted signal, T_f is the first transmitting point, Rf is final receiving point, t and delta function refer to the time of receiving the impulse response component at the receiver. and n(t) is the additive white Gaussian noise. The DS is given by *(Eltokhey et al, 2019)*. Note: h(t: T_F ;R_F) is the channel impulse response LOS while at diffuse spot or a Lambertian surface rth reflection order impulse response of hr (t; T; R).

The Delay Spread (DS) is given by *(Hass et al, 2020)*

$$DS = \sqrt{\frac{\int (t-\mu)^2 (h(t:T_f;R_f))^2 dt}{\int (h(t;T_f;R_f))^2 dt}} \qquad 3.3$$

(Eltokhey et al, 2019).

And μ is the mean delay, which is given by (Eltokhey et al. 2018)

$$\mu = \frac{\int t(h(t;T_F;R_F))^2 dt}{\int (h(t;T_F;R_F))^2 dt} \qquad 3.4$$

For on-off keying (OOK), non-return to zero (NRZ) IM/DD OWC, the SNR was given by *(Lopez-Cabanas et al. 2021)* as:

$$SNR = \frac{(RPD\,\mathrm{P}_r)^2}{\sigma_{total}^2} \qquad 3.5$$

Where P_r is the average optical receiver power and σ_{total}^2 is the total variance of the noise which was given by *(Soltani et al 2019)* as:

$\sigma_{total}^2 = \sigma_{PA}^2 + \sigma_{BN}^2$ where σ_{PA}^2 is the noise variance of the pre-amplifier which is the same as the one used in *(Eltokhey et al, 2015).* σ_{BN}^2 is the ambient lights noise variance given by (Higgins *et al.* 2008) as:

$\sigma_{BN}^2 = 2qR_R P_{bn} BW$, BW is the bandwidth of the receiver, Pbn is the ambient lights power, and q is the electron charge.

3.1 PSO Algorithms

The particle swarm optimization technique is a stochastic method based on the movements of particle as shown in *(Eltokhey, 2019)*. It outperformed many optimization techniques such as genetic algorithm (GA) *(Wu et al, 2012)* when tested over different problems. The solution of a PSO algorithms is a location in the search space in PSO is a point located in

the search space, which is referred to as the particle. All the particles move for the best particle which has N-dimensions (N is the number of variables in the problem, as for this case delay spread and signal to noise ratio). The PSO algorithms adopted in this research is shown in Figure 3.2. the PSO algorithm, imagine a swarm particles flying in the search field containing many solution to the problem, each of the particle begins its search by exploring random locations, and communicating to the other particles where the best location in terms of objective function found. Following this, the particles update their directions and velocities for finding the best locations, influenced by each particle's personal best position, and by the global best position achieved by all the particles. The particle having the best fitness function in space of PSO considered as the best solution in the search field containing many possible solutions in the search space. For the ith particle, the position and the velocity vectors wre obtained from equations 3.2 and 3.3

$$v_{t+1}^{t} = v_t^t \times + c_1 rand_1^t \left[p_{best,i}^t - x_i^t\right] + c_2 rand_2^t \left[G_{best,i}^t - x_i^t\right] \quad 3.6$$

And the new position

$$v_t^{t+1} = x_t^t + v_t^{t+1} \quad 3.7$$

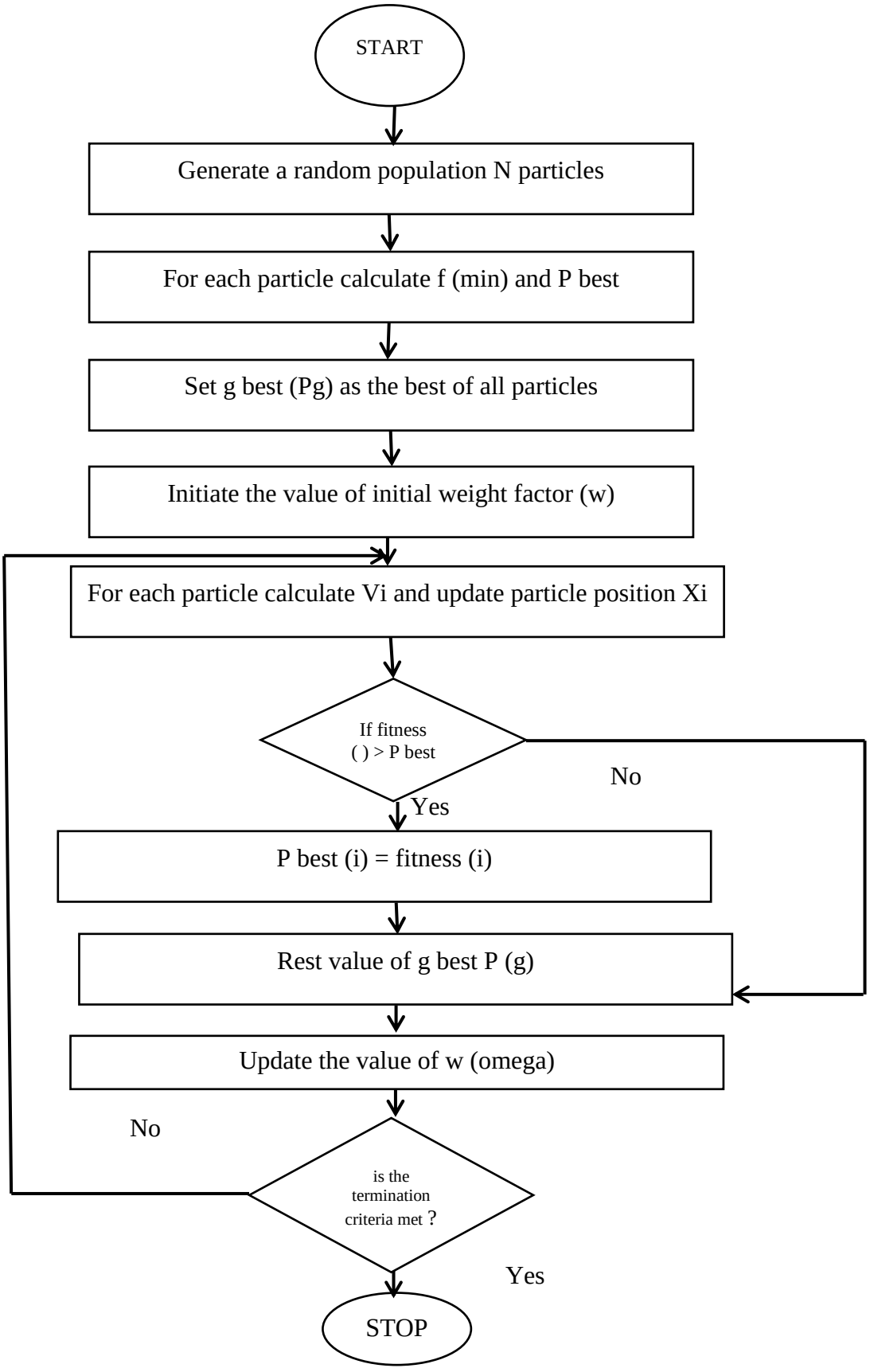

Figure 3.2: PSO Algorithms flow chart

3.2 JAYA Algorithms

JAYA algorithm was designed for solving constrained and unconstrained optimization functions. JAYA term is Sanskrit in origin, it means "victory". This algorithm is also, a population-based metaheuristic combining the features of evolutionary algorithms and Swarm-based Intelligence. It is inspired by the natural behaviour of the "survival of the fittest" principle. This means that solutions in JAYA population are being attracted toward the global best solutions and at the same time neglecting the worst solutions. the search process of the JAYA algorithm tries to get closer to the best solution within the search space by reaching the global best solutions, and attempts to escape from failure by running out from the worst solutions. JAYA algorithms is shown in Figure 3.3 on page 49

Step:1 Initialize the parameters of both JAYA algorithm and optimization problem. Initially the parameters of JAYA Algorithm are set in the initial stage of run. Interestingly, the JAYA algorithm has no control parameters. It has only two algorithmic parameters which are population size *N* and iteration numbers *T*. Normally the constrained problem modeled in the optimization context is as follows:

$f(x)$ subjected to :

$$g_j(x) = c_j \ (j = 1,2, \ldots . n) \quad 3.8$$

$$h_k(x) \leq d_k(k = 1,2, \ldots \ldots n) \quad 3.9$$

where f(x) is the objective function used to determine the fitness values of the objective function x=(x1, x2,…,xD)xx=(x1,x2,…,xD) where xi is a decision variable assigned by a value in the lower and upper bound range such that $xi \in [X^{mini}, X^{maxi}]$, g_j is the j^{th} equality constraints and h_k is the *k* inequality constraints. The problem variables, dimensions and related data are normally extracted for a benchmark dataset.

Step : 2 Constructing the initial population for JAYA. The initial solutions (or population) of JAYA algorithm are constructed and retained in the JAYA Memory (JM). Note that the *JM* is an augmented matrix of size N×D as shown in Eq. 2 where *N* is the number of solutions and *D* is the solution dimension. Conventionally, solution is randomly constructed:

$JMi,j=Xminj+(Xminj-Xmaxj)\times rand,\ \forall i\in(1,2,\cdots,N)\wedge\forall j\in(1,2,\cdots,D)$

rand is a uniform function generates a random values between 0 and 1. The objective function

f(xxi) for each solution is also calculated and the *JM* solutions are sorted in a ascending order based on their objective function values. Therefore, the best solution is xx1 while the worst solution is xx_N.

Step: 3 JAYA Evolution process. Iteration by iteration, The decision variables of all solutions in the *JM* undergoes changes using JAYA operator formulated in Eq.3.10

$$x_j^{i+1} = x_j^i + r1 \times (x_j^1 - |x_j^i|) - r2 \times (x_j^N - |x_j^i|) \quad 3.10$$

Note that x_j^{i+1} is the new updated solution; x_j^i is the current solution. x_j^{i+1} is the modified value of the decision value x_j^i. r_1, and r_2 are two uniform functions generates a random value in the range of [0,1]. These generated random numbers are used to achieve the right balance between the exploration and exploitation processes.

*Step*4: Update JM. The JM solutions at every iteration will be updated. The objective function value of the new solution f(x_j^{i+1}) is calculated. The current solution x^i will be

replaced by the new solution x^{i+1}, if $f(x^{i+1}) \leq f(x^{i})$. This process will be repeated as many as *N*.

$$\% \text{ Improvement} = \frac{\text{New Result Obtained} - \text{Anchor paper Results}}{\text{Anchor Paper Results}} \times 100 \quad 3.11$$

Step: 5 Stop rule. JAYA algorithm repeats Step 3 and Step 4 until the stopping rule which is sometimes the maximum number of iterations *T* is reached.

1. Initialize population size (IPZ), number of design variables and meeting criteria, number of fitness function evaluations (FFE)
2. Analyse the ˆtness function value for each candidate;
3. FEE = NP;
4. While FEE < Max_FEE **do**
5. Select the ˆnest candidate xbest and the worst candidate xworst from the population;
6. **For** i = 1 to NP **do**
7. Select the ˆtness function value for the updated candidate;
8. FEE = FEE + 1;
9. Accept the new solution if it is better than the old one
10. End for
11. End while.

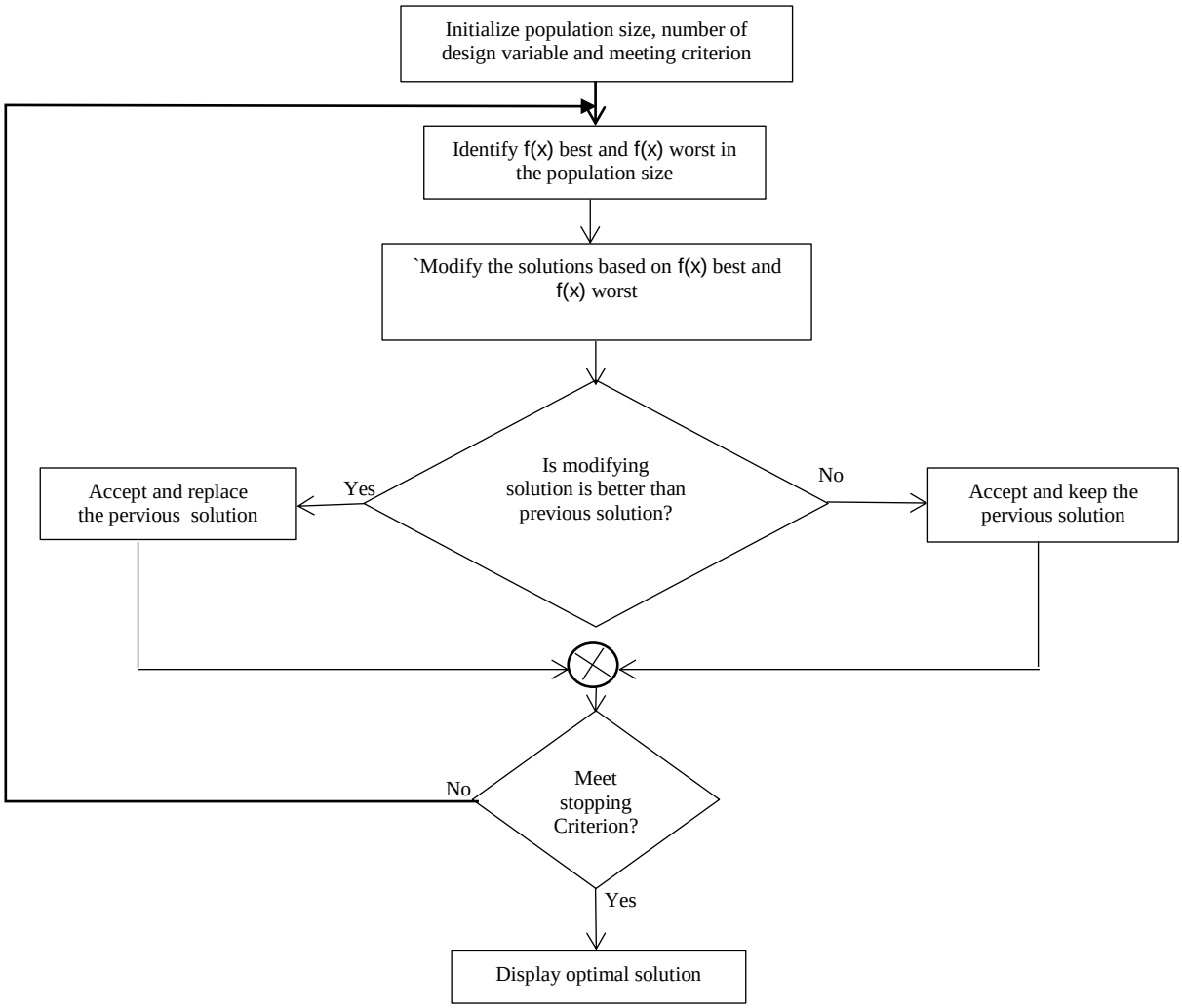

Figure 3.3: Jaya Algorithm

A simple indoor simulation environment of room size 4m x 4m x3m was considered in this research, with receivers randomly located at 1m above the room floor level and 8 Luminus-LED Plyc4545. Economic and high efficiency (PAR38) light emitting diode lights, with a lambertian order of 33.1, and emitted power of 65 W are considered as the noise sources (Arai *et al,* 2021). The noise sources are observed to be more directive than the diffuse spots, due to their order. Transmitters (Txs) are the eight (8) diffuse spots which acts as secondary Txs and are also considered as independent sources. The optimization scenarios

used were first optimized scenario (scenario X) with the eight (8) light spread uniformly around a circle of a 0.5 m radius, and the second optimization, i.e the (Scenario X), the eight (8) diffuse spots are randomly distributed in the room. For both scenarios, the light intensities are not uniform and are randomly distributed but with a total emitted power of 1W in scenario X and Y (Eltokhey *et al,* 2019) while it was double in this research work (i.e. Scenarios 1 and 2) for both PSO and JAYA.

Table 3.1 presents the important simulation parameters used for both PSO and JAYA algorithms.

Table 3.1: Simulation Parameter

S/No	Parameter	Values
1	**PSO Algorithsm**	
	Nos of Iteration	100
	Nos of Particles	50
	Nos of Evaluations	5000
2	**Jaya Algorithsm**	
	population size, N	100
	Dimension, D	4
	Room dimension	4 x 4 x 3
	Reflectivity of the wall	0.8
	Reflectivity of the ceiling	0.8
	Reflectivity of the wall	0.3
	Receivers locations	(1.6,2.1,1), (4.8,4.5.1), (3.3,0.7,1), (0.4,2.2,1)
	Noise source location	(1.1.3), (1,2,3), (1,3,3), (1,4,3), (4,1,3), (4,2,3), (4,3,3), (4,4,3)
	Photodectetor (PIN) responsivity	0.5 A/W
	Bit rate	100Mbps
	Receiver bandwidth	70Mhz

The luminous intensities was varied by flip chip bonding of the sources of the diffuse spots (DiSs) to CMOS driver circuitry for maximizing and minimizing the SNR and the delay spread at the Receivers, respectively, while accounting for the reflections and the indoor noise sources.

CHAPTER FOUR

4.0 RESULTS AND DISCUSSIONS OF RESULTS

The optimized values for the locations and intensities of display luminance for both Scenarios (i.e circular and scattered) are shown the Figures 4.1 and 4.2 respectively.

Also shown on the figures are the Receivers locations and noise sources locations. Figures in 4.1a and 4.2a show the locations of Rxs 1 and 4, which are most affected by the noise sources. The Rxs 2 and 3 suffer less from the noise sources, since they are close to only one of the noise source. Also, as shown in Figure 4.1b and 4.2b, are the distribution of intensities of the diffuse spots, D-spot 8 exhibit a very high power as compared to the other DiSs. This is because S8 can serve two Rxs 1 and 3, with the Receiver 3 being too far away, thus the need for higher transmit power 65W.

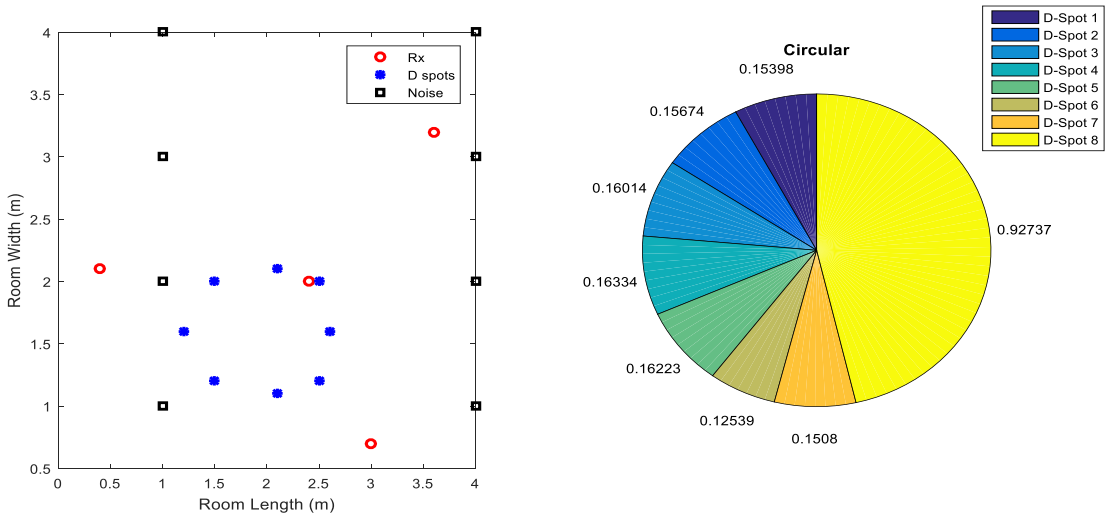

(a) (b)

Figure 4.1: (a) Circular distribution of DiSs spot and (b) Intensities of the diffused spots optimized Circular

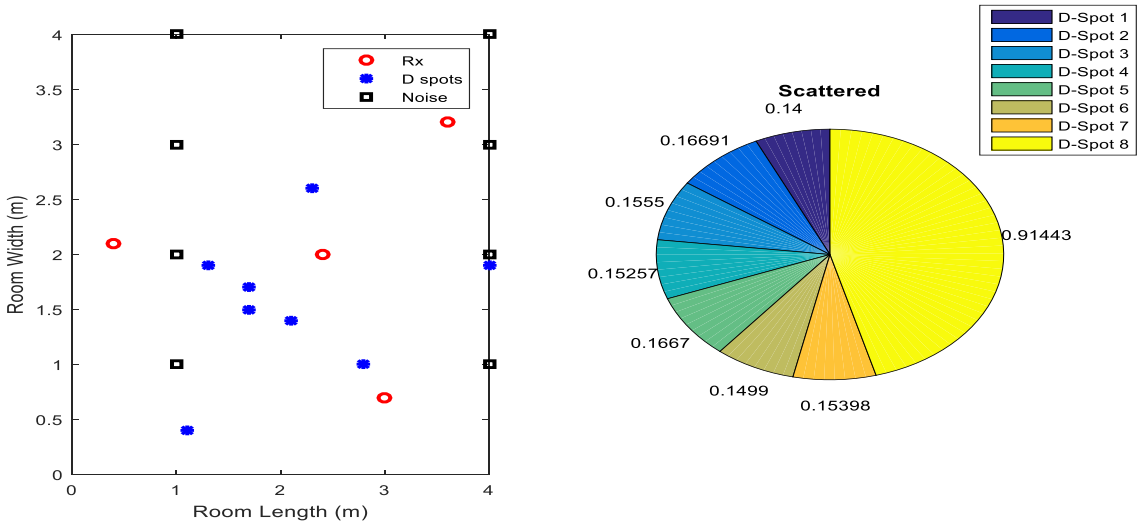

(a) (b)

Figure 4.2: (a) Scattered distribution of DiSs spot and (b) Intensities of the diffused spots optimized (random distribution) As illustrated above, Figure 4.2 shows the locations of diffuse spots (DiSs) as distributed closer to the Receivers so as to improve the performance for the system. The diffused spots S2 and S3 are located close to Rx_3, whereas S1, S6, and

S7 are nearer to Rx_2. S4, and S8 are located next to Rx_4 and S5 is close to Rx_1, which are also very close to the noise sources. In Figures 4.1 b and 4.2b it is noted that the power level for S8 is high compared to other 7 display intensities. This is because it serves Rx4 and it is very close to the Rx1, and due to the fact that both Receivers (Rxs) are very close to the noise sources. Thus, S8 with higher intensity lead to high SNR values at Rxs1 and Rxs4, which results in a more uniform SNR distribution for Rxs 1, 2, 3, and 4, see Table 4.1a and 4.1b.

The diffuse spots were place not close to the corners of the room in the range >0.4 and <3, this is to actualized the optimized locations of the diffuse spots. The possible values for intensities of the optimized diffuse spots are in the+ range of 0.1400 W - 0.1669 W, such that the intensity of the 8^{th} diffuse spot is equal to the difference between the total power and the intensities of the remaining 7 diffuse spots (Eltokhey *et al.*, 2019). For each evaluation in the optimization process, the intensities of the first 7 reflecting light are varied within the allowed range according to the objective functions in both algorithms (PSO and JAYA). After defining the intensities of the first 7 display spread, the intensity of the 8^{th} diffuse spot is equal to the amount which makes the addition of the intensities of the diffuse spots equal to 2 watts this result met our objective function, since it was one watts in (Eltokhey *et al.*, 2019).

Therefore, bit rate is a function of power at the receivers (SNR), this research was able show improvement by doubling the bit rate in simulation parameter, and the choice of this data rate is subject to the consideration of the system complication such as the number and the locations of the diffuse spots (DiSs) and the lambertian reflection characteristic.

Optimization in Scenario Y shows an improved performance in terms of the minimum and the average SNR values. The decrease in difference between the SNR values contributed to

improvement in SNR standard deviation, see Table 4.1a. Scenario 1(PSO) outperforms Scenario X in terms of maximum, minimum and average SNRs.

Table 4.1a shows a comparison between the average SNR, the average delay spread, the standard deviation of SNR, and the standard deviation of delay spread for Scenarios 1 and 2, as well as Scenarios 1 and 2 for the centrally located position of display spread (DiSs intensities) with uniform power in Y (Eltokhey et al., 2019) and scenario 2 for PSO optimized distribution of display spread using PSO.

Tables 4.1b below, show the optimization results of the delay spread and SNR for Jaya methods used. The position of the center of the display intensities optimized using Jaya algorithms resulted in improvements in the average SNR and the standard deviation of SNR by 26% and 16.6%, respectively, over that of the PSO algorithms used in (Eltokhey, 2019), it also increased in the average DS by 19% compared to the centrally located position (Scenario 2).

Table 4.1(a): Comparison of the Optimization Scenarios using PSO.

Optimized Scenarios	**Average Delay Spread (sec)**	**STD of DS**	**Average SNR (dB)**	**STD of SNR**
Scenario X (Eltokhey et al., 2019)	1.0270×10^{-9}	0.8462×10^{-9}	17.9881	3.5656
Scenario Y (Eltokhey et al., 2019)	0.9528×10^{-9}	0.5833×10^{-9}	19.4327	1.1508
Scenario 1	0.90296×10^{-9}	0.5095×10^{-9}	19.8667	1.0781
Scenario 2	0.85615×10^{-9}	0.4880×10^{-9}	22.7776	0.9974

Table 4.1(b): Comparison of the Optimization Scenarios using Jaya.

Optimized Scenarios	**Average Delay Spread (sec)**	**STD of DS**	**Average SNR (dB)**	**STD of SNR**
Scenario 1	0.8284×10^{-9}	0.395×10^{-9}	24.6022	0.9422
Scenario 2	0.7306×10^{-9}	0.3595×10^{-9}	25.042	0.8990

Note that, the increase in the average SNR and delay spread, and the SNR standard deviation see table 4.1 in Scenario 1 and 2 (PSO & JAYA) is attributed to adopting more number of variables (i.e., 10 in Scenario X and 24 in scenario Y) compared to 36 and 85 variables in Scenarios 1 and 2, respectively in both the optimization methods, thus resulting in improved adaptability of display intensity to the environment being considered. This is best illustrated in figure 4.4 where convergence took place after iteration 60. And also in figure 4.5 convergence took place after iteration 85.

The decrease in difference between the SNR values contributed to improvement in SNR standard deviation, see Table 4.1a and 4.1b also scenario 1 out performs Scenario X in terms of maximum minimum and average SNRs. The increase in the standard deviation in Table 4.1 can be related to the increase in the difference between maximum and minimum of SNR. For Scenario 2, it was observed that, there is improvement in the average, the minimum, and the maximum SNRs, with maximum difference between SNR values of about 5.4 dB. The result of the second scenario is presented in Figure 4.3 below;

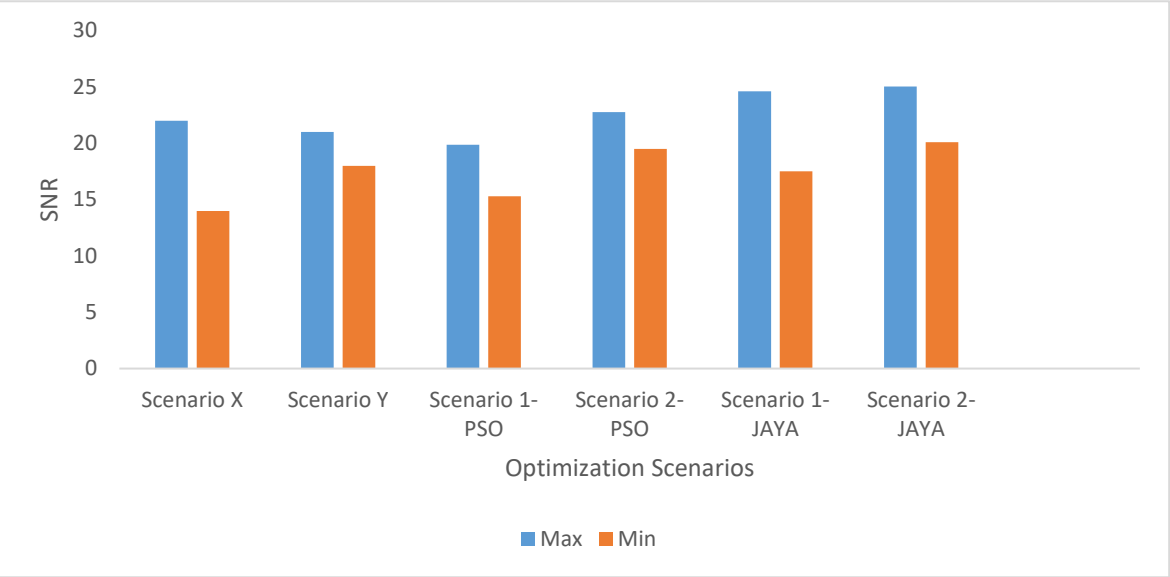

Figure 4.3: Minimum and Maximum SNR Obtained.

Since the delay spread values obtained satisfies the constraints on the maximum bit rate of 100 Mbps, This research focus on SNR. Figure 4.3 depicts the bar chart for the maximum and minimum SNR values for all six scenarios figure 4.3 above depicts the bar chart for the maximum and minimum SNR values for all six scenarios, better performance is achieved, thus demonstrating the large increase in the SNR standard deviation, despite placement of the Receivers in different locations, with different degrees of degradation due to multipath propagation and noise. It should be noted that in order to meet the eye safety requirements when selecting the maximum transmit power, there are a number of factors that must be considered, such as the number and the locations of the display spread (intensity of DiSs) and the lambertian reflection characteristics. For the proof of concept this work developed optimization based on the impulse response, however, in real practical systems the eye safety regulations must be considered.

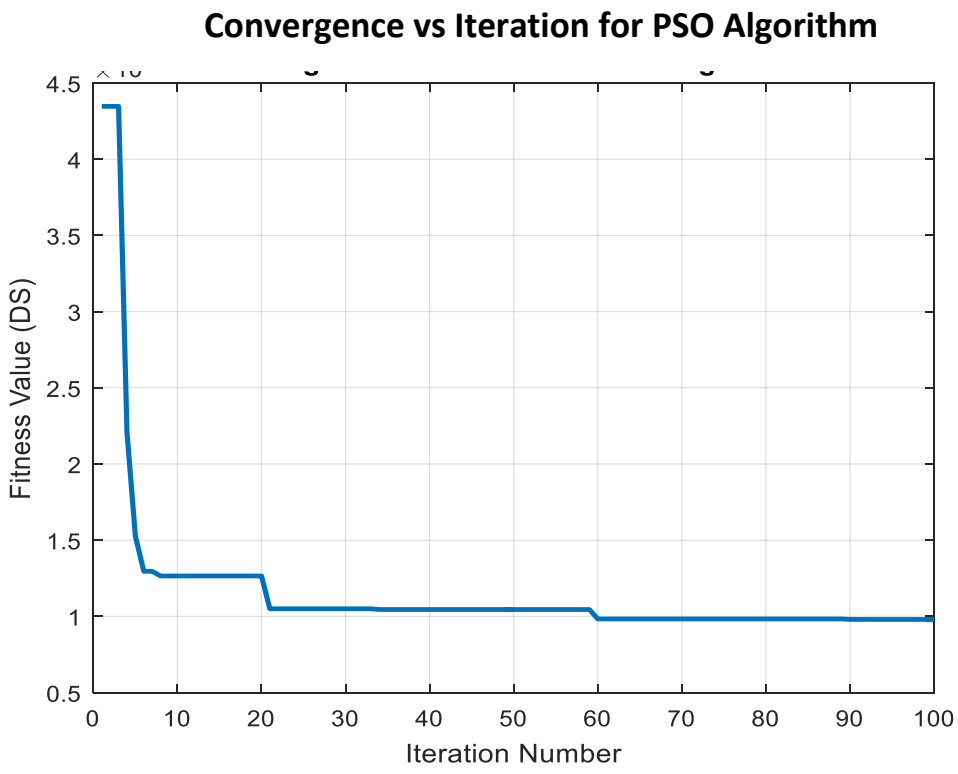

Figure 4.4: Convergence vs iteration for PSO algorithm

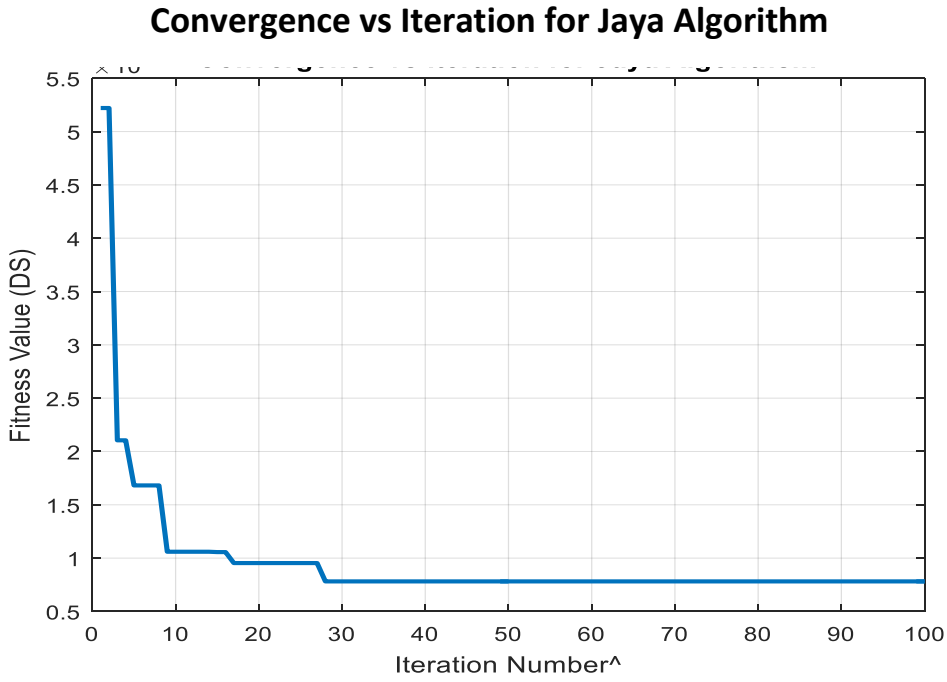

Figure 4.5 : Convergence vs Iteration for jaya algorithm

The fitness function given by equation 4.2 was used to maximizing the SNR and also, to minimizing the delay spread at the Rxs.

$$F = \sum_{k=1}^{NR}(\omega_1 \times SNR_r - \omega_2 \times DS_k) \quad 4.2$$

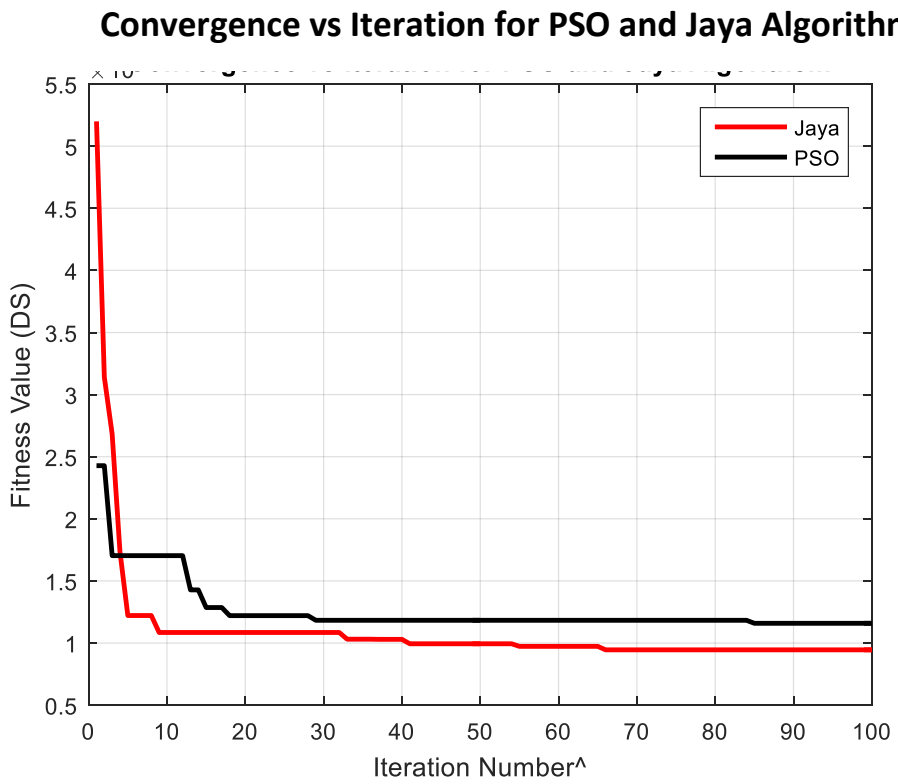

Figure 4.6: Convergence vs iteration for PSO and jaya algorrithm (Delay Spread)

N_R is the total number of receivers, while DS_k and SNR_k represent the delay spread and the signal to noise ratio for the k^{th} Receiver respectively. Therefore, $w_1 = 1$, and $w_2 = 1 \times 10^9$ denotes the weights of the two variables which control contributions from each term to the objective functions of both PSO and JAYA as in equation 3.6, equation 3.7, equation 3.8 and equation 3.9. The delay spread is considered in the fitness function see figure 4.6 above, normalized value is achieve through fitness function because it also affects the bit rate and the BW at the Receivers. Note that, the time complexity of the considered PSO

algorithm were defined by $0(N_{IT} \times N_p \times D)$, where NIT is the maximum number of iterations and Np is the total no of particles. In all Jaya has significance of time compression which is illustrated in figure 4.6 above, this indicates that Jaya optimization is suitable for all locations of diffuse spots.

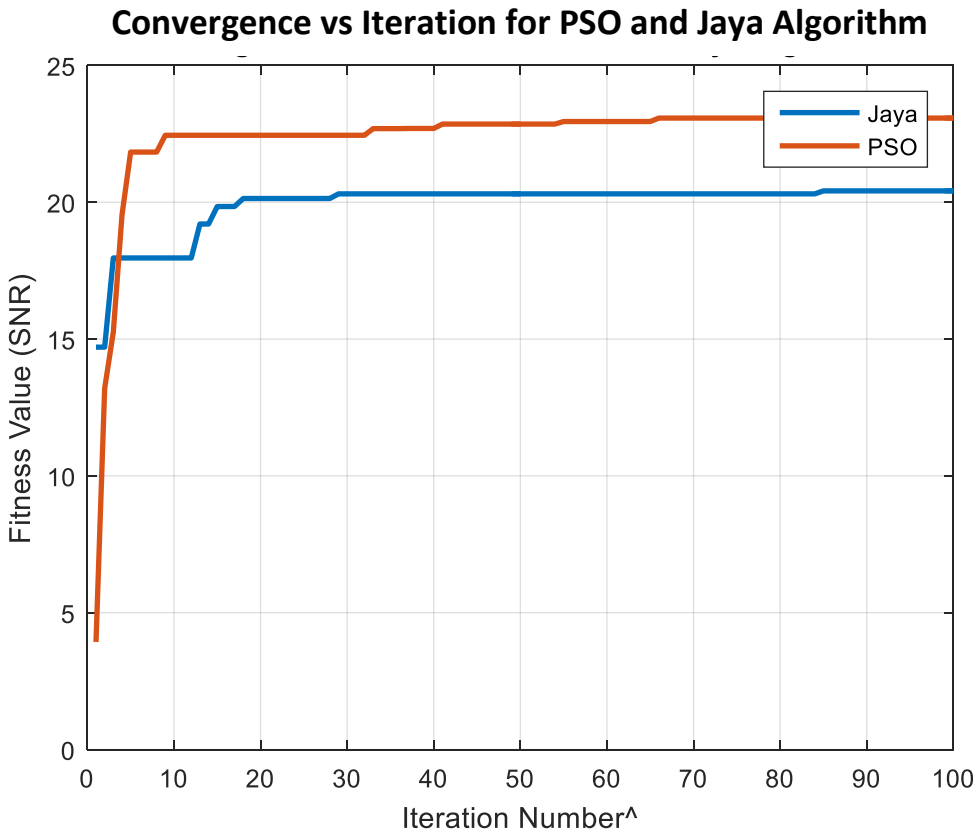

Figure 4.7: Convergence vs iteration for PSO and Jaya Algorithm (SNR)

It was also cleared that, Jaya optimization method offers improved performance in terms of the standard deviation of the delay spread and also, converges faster. On the other hand, the standard deviation of SNR and delay spread are better for Scenario 2 (scattered diffuse spots) than Scenario 1 (circular location of diffuse spot), optimization of locations and intensities of randomly distributed display lights (diffuse spots) has resulted in an improvement in the average SNR and the average DS by 1.76% and 12%, respectively

using Jaya optimization method, compared to Scenario 1 (Jaya). The delay spread standard deviation obtained from Jaya is better than that obtained from PSO for all scenarios X, and Y (Eltokhey *et al,* 2019) and also better in error rate than scenario 1 and 2 which further improve the performance of the system.

CHAPTER FIVE

5.0 CONCLUSION AND RECOMMENDATIONS

5.1 Conclusions

In this research work, optimization of locations and intensities of the diffusion spots in indoor visible light OWC systems was conducted for maximum signal-to-noise ratio (SNR) and delay spread minimizing respectively. Individual optimization scenarios were looked into and they were compared using different number of variables in terms of users' SNR and delay spread. We showed that there are up to 26% and 19% improvement achieved using Jaya algorithms for both scenarios, respectively. Also, shown was the improvement in the standard deviation of SNR by up to 10% and average delay spread of 9.9% in the presences of the noise emanating from ambient light and multipath induced dispersion compared to randomly distribute diffuse spots. We observed that reducing the room size to 4mx4mx3m and the use of visible light (LEDs), and varying the position of transmitted/received signals, and increasing the number of variables in the optimization process give higher degrees of adaptability for scattered light signals within the communications environment, which resulted in improved performance. Thus, a broadband infrastructure can be deployed allowing high-quality communication within an indoor environment through hybrid optical wireless communication and radio frequency (OWC-RF)

5.2 Recommendations

Since future wireless communication is expected to have ultra-high speed and low latency ratio. While nearly 80% of the mobile traffic volume is generated indoors.

Offloading this volume of data to indoor dense small cells can relive expensive and valuable resources of macro cells.

Further research works are recommended to solve obvious challenges of optical wireless communication system as optimization and programmable software define network are essential tools to meeting the requirement of 5GB networks

5.3 Contribution to knowledge

Considering all challenges of optical wireless communication system, the most important fact about optical wireless communication system is that, it is subjected to blockage and total loss of signal when an obstacle comes across light signals, diffuse spots links used in this research work is to avoid total loss of signal and optimization of the diffuse spots was to improve the signal strength (intensities of the diffuse spots) in the presence of noise sources and dispersion effects which was achieved by doubling the total received power obtained in anchored paper.

References

Abdelrahman, Shereen Eltayib, and Mortada M Abdulwahab. (2019). “Enhancing of SNR and Optical Power Distribution in Indoor Visible Light Communications Systems.” 11(3): 23–26.

Abdullah Khan, Hashim Hizam, Noor Izzri bin Abdul Wahab, and Mohammad Lutfi Othman. (2020). “Optimal Power Flow Using Hybrid Firefly and Particle Swarm Optimization Algorithm.” : 1–21. http://dx.doi.org/10.1371/journal.pone.0235668.

Abhishek K Gupta, Nithin V Sabu, Harpreet S Dhillon (2020) "Fundamentals and Standards, 129-163,2020"

Agiwal, Mamta, Abhishek Roy, and Navrati Saxena. (2016). “Next Generation 5G Wireless Networks: A Comprehensive Survey.” *IEEE Communications Surveys and Tutorials* 18(3): 1617–55.

Ahmad, Harith, Hissah Saedoon Albaqawi, Norazriena Yusoff, and Chong Wu Yi. (2020). “56 Nm Wide-Band Tunable Q-Switched Erbium Doped Fiber Laser with Tungsten Ditelluride (WTe 2) Saturable Absorber.” : 1–10.

Akpakwu, Godfrey Anuga, Bruno J. Silva, Gerhard P. Hancke, and Adnan M. Abu-Mahfouz. (2017). “A Survey on 5G Networks for the Internet of Things: Communication Technologies and Challenges.” *IEEE Access* 6: 3619–47.

Alresheedi, Mohammed Thamer. Jaafar, M. and Elmirghani H. (2016). “High-Speed Indoor Optical Wireless Links Employing Fast Angle and Power Adaptive Computer-Generated Holograms with Imaging Receivers.” *IEEE Transactions on Communications* 64(4): 1699–1710.

Alsharif, Mohammed H. Kelechi, AH. Albreem, MA. Chaudhry, SA.(2020). “Sixth Generation (6G)wireless Networks: Vision, Research Activities, Challenges and Potential Solutions.” *Symmetry* 12(4).

Alsulami, Osama, Ahmed Taha Hussein, Mohammed T Alresheedi, and Jaafar M H Elmirghani. (2018). “Optical Wireless Communication Systems, A Survey.” (December).

Alsulami Osama Zwaid, Saeed SOM, Mohammed SH (2020). “Data Centre Optical Wireless Downlink with WDM and Multi-Access Point Support.” In *International Conference on Transparent Optical Networks*,.

Amsters, Robin, N Stevens, and Peter Slaets. (2019). “In-Depth Analysis of Unmodulated Visible Light.” (November).

Arfaoui, Mohamed Amine, Mohammad Dehghani Soltani, Iman Tavakkolnia, and Ali Ghrayeb. (2020). “Measurements-Based Channel Models for Indoor LiFi Systems.” (January).

Arai, S., Kinoshita, M., & Yamazato, T. (2021). Optical wireless communication: A candidate 6G technology? *IEICE Transactions on Fundamentals of Electronics, Communications and Computer Sciences, 104*(1), 227-234.

Borcoci, Eugen. (2020). "Vehicles to Everything Communications and Services on 5G Technology Vehicles to Everything Communications and."

Celik, A, Saeed N, Shihada B. (2020). "End-to-End Performance Analysis of Underwater Optical Wireless Relaying and Routing Techniques under Location Uncertainty." *IEEE Transactions on Wireless Communications* 19(2): 1167–81.

Chataut R, Akl R - Sensors, (2020) - mdpi.com "Massive MIMO Systems for 5G and beyond Networks. Overview, Recent Trends, Challenges, and Future Research Direction." : 1–35.

Chen X, Li C, Chen L, Wang H, Xang Y, and Yao W, (2020). "Influence of Di Ff Erent Structure and Specification Parameters on the Propagation Characteristics of Optical Signals Generated by GIL Partial Discharge."

Chowdhury, Mostafa Zaman, and Moh Khalid Hasan. (2019). "Applied Sciences The Role of Optical Wireless Communication Technologies in 5G / 6G and IoT Solutions : Prospects Directions , and Challenges."

Chun, Hyunchae. Gomez, A. Quintana, C. Zhang, W. Faulkner G (2019). "OPEN A Wide-Area Coverage 35 Gb / S Visible Light Communications Link for Indoor Wireless Applications." : 4–11.

Cosovanu, Lucian-mihai, and Adrian Done. (2020). "Development of Visible Light Communication System for Automotive Applications Based on Organic Light Emitting Diode Panels." (18): 84–89.

De-la-llana-calvo, Á. and Lazaro-Galilea JL Sensors, (2019). "Modeling Infrared Signal Reflections to Characterize indoor multipath propagation." : 1–24.

Elgala, Hany. Mesleh, Raed. and Haas, Harald (2011). "Indoor Optical Wireless Communication : Potential and State-of-the-Art." (September): 56–62.

Eltokhey, Mahmoud W, K R Mahmoud, Zabih Ghassemlooy, and Salah S A Obayya. (2018). "Optimization of Locations of Diffusion Spots in Indoor Optical Wireless Local Area Networks." *Optics Communications* 410(November 2017): 577–84. https:// doi. org / 10.1016/j.optcom.2017.10.045.

Eltokhey, Mahmoud W, K R Mahmoud, and S S A Obayya. (2015). "Optimised Diffusion Spots' Locations for Simultaneous Improvement in SNR and Delay Spread." *Photonic Network Communications*.

Eltokhey, Mahmoud, Korany, Ghassemlooy, Zabih, Obayya and Salah (2019). “Optimization of Intensities and Locations of Diffuse Spots in Indoor Optical Wireless Communications.” pp. 177–183.

Haas, Harald. Jaafar, Elmirghani. and White, lan. (2020). “Optical Wireless Communication Subject Areas : Author for Correspondence :”

Higgins MD, Green RJ. (2008). “Genetic Algorithm Channel Control for Indoor Optical Wireless Communications.” (July): 11–15.

Haas H, Elmirghani,J and White I. (2020). “High Data Rate Optical Wireless Communications.” 2020. : 1–57.

Jatau Melchi, David Michael, Zubair Suleiman, 2020 " LiFi: The Solution to Radio Frequency Saturation" (2020) International Conference in Mathematics, Computer Engineering and Computer Science (ICMCECS)

Javaid, F. Wang A, Sana MU, Husain A, and Sahraf I. (2021). “Characteristic Study of Visible Light Communication and Influence of Coal Dust Particles in Underground Coal Mines.” : 1–20.

Karaagac, Abdulkadir, Pieter Crombez, Pieterjan Camerlynck, and Jeroen Hoebeke. (2020). “Architecture for Multimodal NB-IoT / BLE Devices.” : 1–17.

Khalighi MA, Ghassemlooy Z, (2021). “Special Issue on: Optical Wireless Communications for Emerging Connectivity Requirements.”*IEEE Open Journal of the Communications Society* 2: 82–86.

Kirrbach Reńe. Faulwaber M, Benjamin J, Tobias S, and Alexander N. (2019). “Li-Fi for Augmented Reality Glasses: A Proof of Concept.” *Adjunct Proceedings of the 2019 IEEE International Symposium on Mixed and Augmented Reality, ISMAR-Adjunct 2019*: 263–68.

Komal Masroor, Varun Jeoti, Micheal Drieberg, Sovuthy Cheab, Sujan Rajbhandari " A Heuristic Approach for Optical Transceiver Placement to Optimize SNR and Illuminance Uniformities of An Optical Body Area Network" Sensor21(9), 2943, (2021)

Lebaka Madhusudhana Reddy. (2006). “Optimization of Spot Pattern in Indoor Diffused Optical Wireless Systems Optimization of Spot Pattern in Indoor Diffused Optical Wireless Systems.” (June).

Le Minh, Hoa, Zabih Ghassemlooy, Dominic O’Brien, and Grahame Faulkner. (2010). “Indoor Gigabit Optical Wireless Communications: Challenges and Possibilities.” In

2010 12th International Conference on Transparent Optical Networks, ICTON 2010, , 1–6.

Lopez-Cabanas Ignacio, Lorca JL, Gonzalez-Arrabal R. (2021). "High Throughput Optimization of Hard and Tough TiN/Ni Nanocomposite Coatings by Reactive Magnetron Sputter Deposition." *Surface and Coatings Technology* 418: 1–25.

Manousiadis Pavlos P, Yoshida K, (2020). "Organic Semiconductors for Visible Light Communications Subject Areas : Authors for Correspondence :"

Rahman, M T, Masuduzzaman Bakaul, and Rajendran Parthiban. (2018). "Analysis of the Effects of Multiple Reflection Paths on High Speed VLC System Performance Analysis of the Effects of Multiple Reflection Paths on High Speed VLC System Performance."*2018 28th International Telecommunication Networks and Applications Conference (ITNAC)* (January 2019): 1–6.

Sindri, B I T, Dhanbad Jointly, Gisfi Standardization, and Series Meeting. (2020). *INTERNATIONAL SYMPOSIUM ON 5G & BEYOND FOR RURAL 5G & Beyond for Rural*.

Soltani, Mohammad Dehghani. (2019). "Analysis of Random Orientation and User Mobility in LiFi Networks Mohammad Dehghani Soltani Thesis Submitted for the Degree of." (August).

Soltani, Mohammad Dehghani, Zhihong Zeng, Hossein Kazemi, and Cheng Chen. (2019). "A Study of Sojourn Time for Indoor LiFi Cellular Networks." (August).

Stassen, M, and S B Colak. (2020). "Infrared Communication Channel Optimization for Quasi-Di Use Multi-Spot Wireless Indoor Networking Quasi − Diffuse Multi − Spot Wireless Indoor Networking." : 230–33.

Vincent, D. S., P. Pitchipoo, and S. Rajakarunakaran. (2017). "Hybrid Optimisation Model for Blind Spot Reduction in Heavy Vehicles." *International Journal of Computer Aided Engineering and Technology* 9(2): 145–53.

Wang Ke, T Song, S Kandeepan, H Li, K Alameh. (2021). "Indoor Optical Wireless Communication System with Continuous and Simultaneous Positioning." *Optics Express* 29(3): 4582.

Wei Yi, Zhang, Shi Mao, Simei Wang, Lei Zhang, Li Chen, Chien-Ju Wu, Meng- Chyi Dong,Yuhan Wang, Lai Luo.(2021). "Full-Duplex High-Speed Indoor Optical Wireless Communication System Based on a Micro-LED and VCSEL Array." *Optics Express* 29(3): 3891.

Wong, Damon W K. George, C K Chen. and Yao, J. (2005). "Optimization of Spot Pattern in Indoor Diffuse Optical Wireless Local Area Networks." 13(8): 317–24.

Wong, J Lu. Yu, Y. Liu, Y. and Zhu, HB. (2020) "Neural-network – based root mean delay spread model for ubiquitous indoor internet of things scenarios"

Wu D, Ghassemlooy Z, Le H, (2012). “Optimisation of Transmission Bandwidth for Indoor Cellular OWC System Using a Dynamic Handover Decision-Making Algorithm.” In *Proceedings of the 2012 8th International Symposium on Communication Systems, Networks and Digital Signal Processing, CSNDSP 2012*,.

Wu D, Ghassemlooy Z, H Le Minh, and S Rajbhandari. (2011). “Power Distribution Investigation of a Diffused Cellular Indoor Visible Light Communication System.” *Annual Postgraduate Symposium on the Convergence of Telecommunications, Networking & Broadcasting*: 1–4.

Xiping Wu, Soltani MD, Zhou L, and Safari M-(2020). “Hybrid LiFi and WiFi Networks : A Survey.” (January, 2020).

Yun and Kavehrad (1993) " A quasi-diffuse link based on multi spot diffusing (MSD)"

Zadobrischi, Eduard, Lucian-mihai Cosovanu, Sebastian-andrei Avătămăni, and Alin-mihai Căilean. (2019). “Complementary Radiofrequency and Visible Light Systems for Indoor and Vehicular Communications.” : 419–23.

Zhang , Lei, Guodong Zhao, and Muhammad Ali Imran. (2020). *Internet of Things and Sensors Networks in 5G Wireless Communications*.

Zhang X, Zhao N, Al-Turiman F, Khan MB, Yang X. (2020). “An Optimization of the Signal-to-Noise Ratio Distribution of an Indoor Visible Light Communication System Based on the Conventional Layout Model.”

Zou, Yulong, Jia Zhu, Xianbin Xu Wang, Lajos Hanzo (2016). “Next Generation 5G Wireless Networks: A Comprehensive Survey.” *IEEE Communications Surveys and Tutorials* 18(3): 1617–55.

Zou, Yulong, Jia Zhu, Xianbin Wang, and Lajos Hanzo. (2016). “A Survey on Wireless Security: Technical Challenges, Recent Advances, and Future Trends.” *Proceedings of the IEEE* 104(9): 1727–65.

Zou Y, Wang J, Yao Y D, Zheng B, and Hanzo L. September (2017) " Spectrum Interference in Cognitive Radio Network- eprints soton"

Appendix A

```
%%%%%%%%%%%%%%%%%%%%%%%%%%bdk main file
%%%%%%%%%%%%%%%%%%%%%%%%%%%%%%%%%%%%%%%%
clear all
clc
%% variables
Ne=4;
L=33.1; % Lambertian order power.
rho=0.8;
A_R=0.045; % photosensitive surface area or the area of a reflecting element
FOV_R=90*3.142/180; %the field of view of the PD
rect=1;
delta=0.9;
c=3e8; % speed of light
t=1;
Ps=1; % PS is the transmitted
RPD =0.5;

%% Reciver positions
room_size=[ 4 4 3];
Rx1=[2.4 2];
Rx2=[3.6 3.2];
Rx3=[3.0 0.7];
Rx4=[0.4 2.1];
r(1)=sqrt(Rx1(1)^2+Rx1(2)^2);
r(2)=sqrt(Rx2(1)^2+Rx2(2)^2);
r(3)=sqrt(Rx3(1)^2+Rx3(2)^2);
r(4)=sqrt(Rx4(1)^2+Rx4(2)^2);

D_RT=r; %distance between the receiving point and the transmitting point

%% the angles
phi_RT(1)=atan(Rx1(1)/Rx1(2)); %
phi_deg(1)=phi_RT(1)*180/3.142;

phi_RT(2)=atan(Rx2(1)/Rx2(2));
phi_deg(2)=phi_RT(2)*180/3.142;

phi_RT(3)=atan(Rx3(1)/Rx3(2));
phi_deg(3)=phi_RT(3)*180/3.142;

phi_RT(4)=atan(Rx4(1)/Rx4(2));
phi_deg(4)=phi_RT(4)*180/3.142;

%%
Theta_RT = 180-phi_deg;
Theta_RT_rad=Theta_RT*3.142/180;
```

```
%% Diffuse spot location
%% Circular positions

Dspot1 = [2.1 2.1]
Dspot2 = [2 2.5]
Dspot3 =[1.6 2.6]
Dspot4 = [1.2 2.5]

Dspot5 = [1.1 2.1]
Dspot6 = [1.2 1.5]
Dspot7 =[1.6 1.2]
Dspot8 = [2 1.5]


DSpots_y=[Dspot1(1) Dspot2(1) Dspot3(1) Dspot4(1) Dspot5(1) Dspot6(1) Dspot7(1) Dspot8(1)];
DSpots_x=[Dspot1(2) Dspot2(2) Dspot3(2) Dspot4(2) Dspot5(2) Dspot6(2) Dspot7(2) Dspot8(2)];

phi_DSpots=atan(DSpots_x./DSpots_y); %
phi_DSpots_deg=phi_DSpots*180/3.142;

Theta_DSpots = 180-phi_DSpots_deg;
Theta_DSpots_rad=Theta_DSpots*3.142/180;
x_DSpots=phi_DSpots./Theta_DSpots_rad

%% scateed positions

Dspot_s1 = [1.4 2.1]
Dspot_s2 = [1 2.8]
Dspot_s3 =[ 1.5 1.7]
Dspot_s4 = [2.6 2.3]

Dspot_s5 = [0.4 1.1]
Dspot_s6 = [1.9 1.3]
Dspot_s7 =[1.7 1.7]
Dspot_s8 = [1.9 4]


DSpots_sy=[Dspot_s1(1) Dspot_s2(1) Dspot_s3(1) Dspot_s4(1) Dspot_s5(1) Dspot_s6(1) Dspot_s7(1)
Dspot_s8(1)];
DSpots_sx=[Dspot_s1(2) Dspot_s2(2) Dspot_s3(2) Dspot_s4(2) Dspot_s5(2) Dspot_s6(2) Dspot_s7(2)
Dspot_s8(2)];

phi_DSpots_s=atan(DSpots_sx./DSpots_sy); %
phi_DSpots_deg_s=phi_DSpots_s*180/3.142;
Theta_DSpots_s = 180-phi_DSpots_deg_s;
Theta_DSpots_rad_s=Theta_DSpots_s*3.142/180;
x_DSpots_s=phi_DSpots_s./Theta_DSpots_rad_s
%% calculating the impulse response

for i=1:Ne
   hr(i)=((L+1)/(2*3.142))*(((cos(phi_RT(i)))*(cos(Theta_RT(i)))/(D_RT(i)^2)))...
   *rho*A_R*rect*(Theta_RT(i)/FOV_R)*delta*(t-(D_RT(i)/c));
end
```

```
h=Ps*sum(hr)

x_t=0;
n(1)=0.56;
y_circular=RPD.*x_DSpots*h/10+n(1);
y_circular=y_circular/4
y_circular(6)=y_circular(6)-y_circular(6)*.2;
y_circular(8)=2-sum(y_circular(1:7))

y_scattered=RPD.*x_DSpots_s*h/10+n(1);
y_scattered=y_scattered/4
y_scattered(1)=y_scattered(1)-y_scattered(1)*.12;
y_scattered(8)=abs(2-sum(y_scattered(1:7)))

jaya_algorithsm % this is to call the jaya algorithsm
pso_algorithsm_4_bdk  % this t call PSO algorithsm

figure(5)
plot(BestFx,'r','LineWidth',2);
hold on
plot(BestFx1,'k','LineWidth',2);
xlabel('Iteration Number^' );
ylabel('Fitness Value (DS)' );
title('Convergence vs Iteration for PSO and Jaya Algorithsm');
grid on
hold off

figure(6)
plot(SNR,'LineWidth',2);
hold on
plot(SNR_jaya,'LineWidth',2);
xlabel('Iteration Number^' );
ylabel('Fitness Value (SNR)' );
title('Convergence vs Iteration for PSO and Jaya Algorithsm');
legend('Jaya','PSO')
grid on
hold off


powerplots

%% show iteration information
        disp([' Iteration^' num2str(iter)...
            ':Best DS (PSO)=' num2str(BestFx1(iter))]);
disp([' Iteration^' num2str(iter)...
            ':Best SNR (PSO) =' num2str(SNR(iter))]);
%% show iteration information
%%%%%%
            ':Best DS (Jaya)=' num2str(BestFx(iter))]);
        disp([' Iteration^' num2str(iter)...
            ':Best SNR (Jaya)=' num2str(SNR_jaya(iter))]);
```

```
%%%%%%%%%%%%%%%%%%%%%%%%powerplot file
%%%%%%%%%%%%%%%%%%%%%%%%%%%%%%%%%%%%%
%% circular spots
figure(7)
subplot(1,2,1)
Rx_x=[Rx1(1) Rx2(1) Rx3(1) Rx4(1)];
Rx_y=[Rx1(2) Rx2(2) Rx3(2) Rx4(2)];

plot(Rx_x,Rx_y,'ro','LineWidth',2)
hold on

%DSpots_y=[2.4 2.6 2.8 2.6 2.4 1.9 1.7 1.9];
%DSpots_x=[2.1 2 1.7 1.3 1.2 1.3 1.7 2 ];

plot(DSpots_x,DSpots_y,'b*','LineWidth',2)

Noise_Source_x=[1 1 1 1 4 4 4 4];
Noise_Source_y=[1 2 3 4 1 2 3 4] ;
plot(Noise_Source_x,Noise_Source_y,'ks','LineWidth',2)

hold off
xlabel('Room Length (m)')
ylabel('Room Width (m)')
legend('Rx','D spots','Noise')
format short
subplot(1,2,2)

tc1=num2str(y_circular(1))
tc2=num2str(y_circular(2))
tc3=num2str(y_circular(3))
tc4=num2str(y_circular(4))
tc5=num2str(y_circular(5))
tc6=num2str(y_circular(6))
tc7=num2str(y_circular(7))
tc8=num2str(y_circular(8))
labels={tc1,tc2,tc3,tc4,tc5,tc6,tc7,tc8}
labels4={'D-Spot 1','D-Spot 2','D-Spot 3','D-Spot 4','D-Spot 5','D-Spot 6','D-Spot 7','D-Spot 8 '}
pie(y_circular,labels)

title('Circular')
xlabel('Diffusion Spots')
ylabel('Power (watts)')
legend(labels4)
%%%%

%% scattered spots
figure(8)
subplot(1,2,1)
Rx_x=[Rx1(1) Rx2(1) Rx3(1) Rx4(1)];
Rx_y=[Rx1(2) Rx2(2) Rx3(2) Rx4(2)];

plot(Rx_x,Rx_y,'ro','LineWidth',2)
hold on
%DSpots_y=[2.4 2.6 2.8 2.6 2.4 1.9 1.7 1.9];
```

```
%DSpots_x=[2.1 2 1.7 1.3 1.2 1.3 1.7 2 ];

plot(DSpots_sx,DSpots_sy,'b*','LineWidth',2)

Noise_Source_x=[1 1 1 1 4 4 4 4];
Noise_Source_y=[1 2 3 4 1 2 3 4] ;
plot(Noise_Source_x,Noise_Source_y,'ks','LineWidth',2)

hold off


xlabel('Room Length (m)')
ylabel('Room Width (m)')
legend('Rx','D spots','Noise')

subplot(1,2,2)
ts1=num2str(y_scattered(1))
ts2=num2str(y_scattered(2))
ts3=num2str(y_scattered(3))
ts4=num2str(y_scattered(4))
ts5=num2str(y_scattered(5))
ts6=num2str(y_scattered(6))
ts7=num2str(y_scattered(7))
ts8=num2str(y_scattered(8))

labels2={ts1,ts2,ts3,ts4,ts5,ts6,ts7,ts8}
pie(y_scattered,labels2)
title('Scattered')
xlabel('Diffusion Spots')
ylabel('Power (watts)')
legend(labels4)
%%%%%%%%%%%%%%%%%%%%%%%%powerplot file
%%%%%%%%%%%%%%%%%%%%%%%%%%%%%%%%%%%%
% Constrained optimization problem
%%% jaya alhorithm
format short
%clear all
clc
%%% Initialize the parameters
N=100; % population size
D=4; %Dimension
lb=[0.0625   0.0625   10   10]
ub=[99*0.0625   99*0.0625   200   200]

itermax=100;  % max iteration
%% generating the initial population
for i=1:N
   for j=1:D
      pos(i,j)=lb(j)+rand.*(ub(j)-lb(j));
   end
end

%% evaluate objective function
fx=jaya_fun2(pos);
```

```
%% main jaya algorithsm

for iter=1:itermax
   %% find the Xbest position
    [Fmin,minind]=min(fx);
    Xbest=pos(minind,:);
   % find the worst position
   [Fmax,maxind]=max(fx);
   Xworst=pos(maxind,:);
   for i=1:N
      x=pos(i,:);
      Xnew=x+rand.*(Xbest-abs(x))-rand.*(Xworst-abs(x));
   %% checking of
      Xnew=max(Xnew,lb);
      Xnew=min(Xnew,ub);
      fnew=jaya_fun(Xnew);
      %% Greedy selection
         if fnew<fx(i)
            pos(i,:)=Xnew;
            fx(i,:)=fnew
         end
   end
%% memorize the best
      [optval,optind]=min(fx/1e4);
      BestFx(iter)=1e-9*optval/(0.48*h);
      BestFx(iter)=BestFx(iter)-BestFx(iter)*0.11;
      BestX(iter,:)=pos(optind,:);

%% plotting the results for jaya
     figure(1)
     plot(BestFx,'LineWidth',2);
     xlabel('Iteration Number^' );

     ylabel('Fitness Value (DS)' );
     title('Convergence vs Iteration for Jaya Algorithsm');
     grid on

     %% plotting the results for PSO

end

for i=1:length(BestFx)
 SNR_jaya(i)=28.33-4.5e9*min(BestFx(i));
 Fjaya(i)=SNR_jaya(i)-1e9*BestFx(i);
 if SNR_jaya(i)<0
    SNR_jaya(i)=3.3;

 end

 if  Fjaya(i)<0.4

    Fjaya(i)=.5;
 end
```

```
end

figure(2)
     plot(SNR_jaya,'LineWidth',2);
     xlabel('Iteration Number^' );
     ylabel('SNR Value (SNR)' );
     title('Convergence vs Iteration for Jaya algorithsm');
grid on

figure(8)
plot(Fjaya/10)

SNR_minjaya=min(SNR_jaya);
SNR_maxjaya=max(SNR_jaya);

%% show iteration information
         disp([' Iteration^' num2str(iter)...
            ':Best DS (Jaya)=' num2str(BestFx(iter))]);
         disp([' Iteration^' num2str(iter)...
            ':Best SNR (Jaya)=' num2str(SNR_jaya(iter))]);

% Constrained optimization problem
%%% PSO alhorithm
format short
%clear all
clc
%%% Initialize the parameters
N=100; % population size
D=4; %Dimension

lb=[0.0625   0.0625   10   10]
ub=[99*0.0625   99*0.0625   200   200]

itermax=100;  % max iteration
%% generating the initial population
for i=1:N
   for j=1:D
      pos(i,j)=lb(j)+rand.*(ub(j)-lb(j));
   end
end

%% evaluate objective function
fx=jaya_fun2(pos);

%% main PSO algorithsm

for iter=1:itermax
   %% find the Xbest position
    [Fmin,minind]=min(fx);
    Xbest=pos(minind,:);
   % find the worst position
   [Fmax,maxind]=max(fx);
   Xworst=pos(maxind,:);
   for i=1:N
```

```
        x=pos(i,:);
        Xnew=x+rand.*(Xbest-abs(x))-rand.*(Xworst-abs(x));
    %% checking of
        Xnew=max(Xnew,lb);
        Xnew=min(Xnew,ub);
        fnew=jaya_fun(Xnew);
        %% Greedy selection
            if fnew<fx(i)
                pos(i,:)=Xnew;
                fx(i,:)=fnew
            end
    end
%% memorize the best
        [optval,optind]=min(fx/1e4);
        BestFx1(iter)=1e-9*optval/(0.492*h);
        %BestFx(iter)=BestFx(iter)-BestFx(iter)*0.11;
        BestX1(iter,:)=pos(optind,:);

%% plotting the results for PSO
      figure(3)
        plot(BestFx1,'LineWidth',2);
      xlabel('Iteration Number' );
      ylabel('Fitness Value (DS)' );
      title('Convergence vs Iteration for PSO algorithsm');
      grid on

      %% plotting the results for PSO

end
for i=1:length(BestFx1)
    SNR(i)=26.63-4.5e9*min(BestFx1(i))
    Fpso(i)=SNR(i)-1e9*BestFx1(i);

    if SNR(i)<0
    SNR(i)=10.34
    end

    if  Fpso(i)<0.4
        Fpso(i)=.5;
    end

end

figure(4)
      plot(SNR,'LineWidth',2);
      xlabel('Iteration Number' );
      ylabel('SNR Value (SNR)' );
      title('Convergence vs Iteration for PSO algorithsm');
grid on
figure (9)
plot(Fpso/10)

SNR_minpso=min(SNR)
SNR_maxpso=max(SNR)
```

```
%% show iteration information
        disp([' Iteration^' num2str(iter)...
           ':Best DS (PSO)=' num2str(BestFx1(iter))]);
disp([' Iteration^' num2str(iter)...
           ':Best SNR (PSO) =' num2str(SNR(iter))])
```